Cell PRESS

Immunity
Article

The Cytokine RANKL Produced by Positively Selected Thymocytes Fosters Medullary Thymic Epithelial Cells that Express Autoimmune Regulator

Yu Hikosaka,[1,10] Takeshi Nitta,[1,10] Izumi Ohigashi,[1] Kouta Yano,[1] Naozumi Ishimaru,[2] Yoshio Hayashi,[2] Mitsuru Matsumoto,[3] Koichi Matsuo,[4] Josef M. Penninger,[5] Hiroshi Takayanagi,[6] Yoshifumi Yokota,[7] Hisakata Yamada,[8] Yasunobu Yoshikai,[8] Jun-ichiro Inoue,[9] Taishin Akiyama,[9] and Yousuke Takahama[1,*]

[1]Division of Experimental Immunology, Institute for Genome Research
[2]Division of Oral Molecular Pathology, Institute of Health Biosciences
[3]Division of Molecular Immunology, Institute for Enzyme Research
University of Tokushima, Tokushima 770-8503, Japan
[4]Department of Microbiology and Immunology, School of Medicine, Keio University, Tokyo 160-8582, Japan
[5]Institute of Molecular Biotechnology, Austrian Academy of Science, 1030 Vienna, Austria
[6]Department of Cell Signaling, Tokyo Medical and Dental University, Tokyo 113-8549, Japan
[7]Division of Molecular Genetics, Faculty of Medical Sciences, University of Fukui, Fukui 910-1193, Japan
[8]Division of Host Defense, Medical Institute of Bioregulation, Kyushu University, Fukuoka 812-8582, Japan
[9]Division of Cellular and Molecular Biology, Institute of Medical Science, University of Tokyo, Tokyo 108-8639, Japan
[10]These authors contributed equally to this work
*Correspondence: takahama@genome.tokushima-u.ac.jp
DOI 10.1016/j.immuni.2008.06.018

SUMMARY

The thymic medulla provides a microenvironment where medullary thymic epithelial cells (mTECs) express autoimmune regulator and diverse tissue-restricted genes, contributing to launching self-tolerance. Positive selection is essential for thymic medulla formation via a previously unknown mechanism. Here we show that the cytokine RANK ligand (RANKL) was produced by positively selected thymocytes and regulated the cellularity of mTEC by interacting with RANK and osteoprotegerin. Forced expression of RANKL restored thymic medulla in mice lacking positive selection, whereas RANKL perturbation impaired medulla formation. These results indicate that RANKL produced by positively selected thymocytes is responsible for fostering thymic medulla formation, thereby establishing central tolerance.

INTRODUCTION

The thymus provides multiple microenvironments that sequentially support the development and selection of T lymphocytes. Thymocytes that express clonotypic and diverse T cell antigen receptors (TCR) are generated in the thymic cortex where cortical thymic epithelial cells (cTECs) present a set of self-peptides by virtue of proteasomes containing β5t and lysosomal proteases including cathepsin L (Finkel et al., 1989; Honey et al., 2002; Murata et al., 2007). TCR interaction with self-peptide-loaded MHC molecules expressed by cortical cells, including cTECs and hematopoietic cells, determines the life and death of immature thymocytes, and a fraction of cortical thymocytes survive TCR signals for further development (Kisielow et al., 1988; Daniels et al., 2006) and relocate to the thymic medulla chiefly via CCR7-mediated chemotaxis (Ueno et al., 2004; Kwan and Killeen, 2004). This process in the thymic cortex, referred to as positive selection, enriches T lymphocytes that demonstrate modest reactivity to self-peptides and potential responsiveness to foreign antigens. Entering the thymic medulla, positively selected semimature thymocytes further interact with self-peptides that are expressed by medullary thymic epithelial cells (mTECs) and dendritic cells (DCs). mTECs express a diverse set of genes representing essentially all tissues of the body, at least partly because of a nuclear molecule called autoimmune regulator (Aire) (Derbinski et al., 2001; Anderson et al., 2002), whereas thymic DCs, which efficiently present various self-peptides, are predominantly localized in the medulla and at least in part derived from circulation (Bonasio et al., 2006). The interaction of positively selected thymocytes in the thymic medulla with a diverse set of self-peptides, including tissue-restricted antigens presented by mTECs and DCs, is essential for establishing self-tolerance (Gallegos and Bevan, 2004).

Thymic medulla formation is dependent on the differentiation of mTECs from their endodermal precursor cells that are generated at the third pharyngeal pouch (Rossi et al., 2006; Bleul et al., 2006; Hamazaki et al., 2007), and the development of mTECs is regulated by the NF-κB activation pathway that includes transcription factor RelB and signal transducer TRAF6 (Burkly et al., 1995; Boehm et al., 2003; Akiyama et al., 2005). A recent study showed that $CD4^+CD3^-$ lymphoid tissue inducer (LTi) cells are involved in initiating embryonic mTEC development by producing the cytokine RANK ligand (RANKL) (Rossi et al., 2007).

Importantly, generation of the thymic microenvironment is also regulated by the development of thymocytes. This regulation is referred to as thymic crosstalk, and the signals produced by positively selected thymocytes are crucial for thymic medulla formation (Shores et al., 1991; van Ewijk et al., 1994). Mice deficient for the generation of mature thymocytes because of the lack of

positive selection exhibit defective medulla development (Philpott et al., 1992; Negishi et al., 1995), and reconstitution of the thymus with positively selected thymocytes restores formation of the medullary region (Surh et al., 1992; Nasreen et al., 2003). Thymus deficient for positive selection contains scattered and small clusters of mTECs, suggesting that positively selected thymocytes are responsible for the development of mTECs (Naspetti et al., 1997; Gray et al., 2006). Nonetheless, whether positive selection regulates the number or functional maturation of mTECs remains unclear. Molecular signals that regulate positive-selection-mediated medulla formation are also unknown.

The present study was aimed at identifying molecules that participate in positive-selection-mediated medulla formation in the thymus. We show that the interaction between RANKL produced by positively selected thymocytes and RANK and osteoprotegerin (OPG, a decoy receptor for RANKL) expressed by mTECs played a crucial role in positive-selection-mediated medulla formation by regulating the cellularity of Aire-expressing mTECs. We also present evidence that medulla formation in adult mice was chiefly regulated by positively selected thymocytes rather than by other intrathymic RANKL-expressing cells, including LTi cells. Thus, this study demonstrates that RANKL produced by positively selected thymocytes plays a major role in increasing the number of mTECs and forming thymic medulla that contains Aire-expressing mTECs.

RESULTS

Positive Selection Fosters Medulla Formation by Affecting mTEC Cellularity

It was previously shown that positive selection is crucial for thymic medulla formation and that mice lacking positive selection because of a deficiency of either TCRα or TCR-associated tyrosine kinase ZAP70 exhibit defective medulla formation in the thymus (Philpott et al., 1992; Negishi et al., 1995; also shown in hematoxylin-eosin-stained sections of Figure 1A). However, in agreement with previous findings (Naspetti et al., 1997; Gray et al., 2006), the scattered distribution of small mTEC clusters identified by mTEC-specific antibody ER-TR5 and mTEC-binding lectin UEA1 was detectable in the thymus of TCRα-deficient (*Tcra*$^{-/-}$) or ZAP70-deficient (*Zap70*$^{-/-}$) mice (Figure 1A). Flow cytometry analysis of thymic stromal cells showed that the numbers of mTEC identified as CD45$^-$I-A$^+$UEA1$^+$ or CD45$^-$I-A$^+$Ly51$^-$ were markedly reduced in TCRα-deficient or ZAP70-deficient mice (approximately 5%–10% of normal numbers), whereas the numbers of cTEC identified as CD45$^-$I-A$^+$UEA1$^-$ or CD45$^-$I-A$^+$Ly51$^+$ were not considerably reduced (Figures 1B and 1C). These results indicate that positive selection affects the number of mTECs but not of cTECs.

The major function of mTECs so far identified is to establish central tolerance by expressing a diverse set of tissue-restricted genes and by attracting positively selected cortical thymocytes for interaction with mTECs and DCs in the medulla (Derbinski et al., 2001; Anderson et al., 2002; Ueno et al., 2004; Kwan and Killeen, 2004; Gallegos and Bevan, 2004; Bonasio et al., 2006). Molecules involved in this mTEC function include Aire, a nuclear factor associated with promiscuous gene expression (Anderson et al., 2002), and CCL21, a chemokine that attracts positively selected thymocytes that express CCR7 (Ueno et al.,

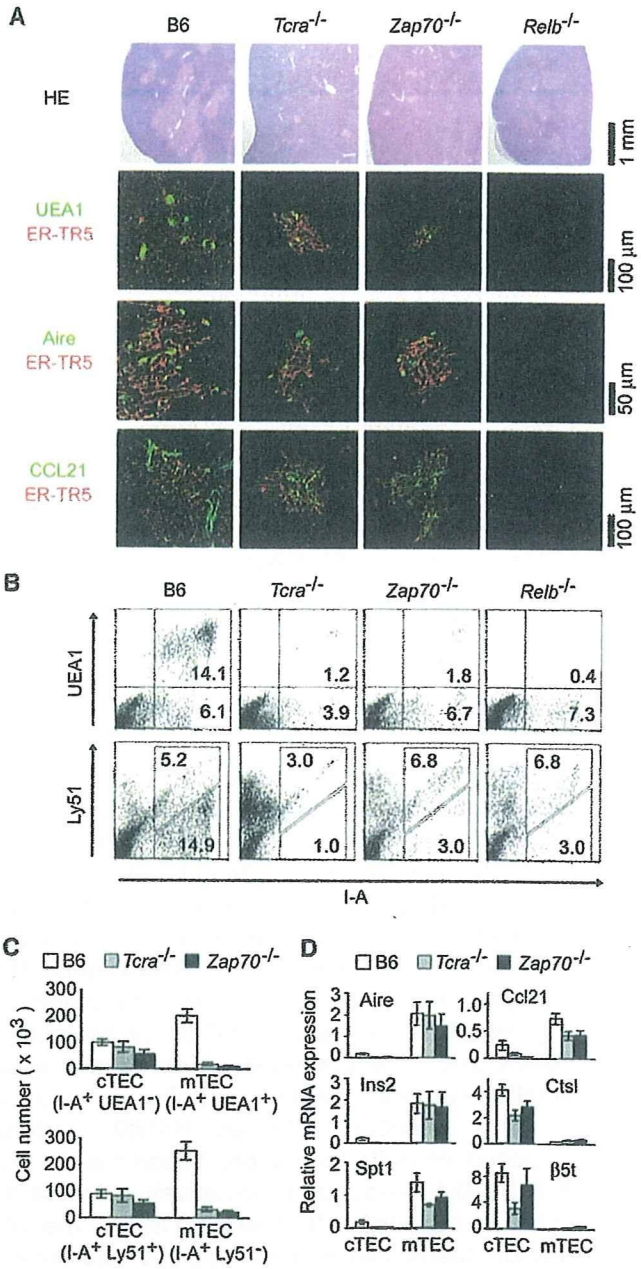

Figure 1. Positive Selection of Thymocytes Affects Number of mTECs

(A) Thymus lobes from 4- to 6-week-old young adult B6, *Tcra*$^{-/-}$, *Zap70*$^{-/-}$, or *Relb*$^{-/-}$ mice were stained with hematoxylin and eosin (HE) or with mTEC-specific monoclonal antibody ER-TR5 (red) and UEA1, antibody specific for Aire, or antibody specific for CCL21 (green).

(B) Two-color flow cytometry profiles for I-A and UEA1 (top) and I-A and Ly51 (bottom) of CD45$^-$ nonleukocytes prepared from thymuses of 4- to 6-week-old mice. Numbers indicate frequency of cells within indicated areas.

(C) Numbers of cTECs and mTECs per mouse in indicated mice. Averages and standard errors (B6, n = 4; *Tcra*$^{-/-}$, n = 4; *Zap70*$^{-/-}$, n = 3) are shown.

(D) Quantitative RT-PCR analysis of indicated genes in isolated cTECs and mTECs. mRNA expression was normalized to GAPDH mRNA, and those in CD45$^-$ total thymic stromal cells were arbitrarily set to 1. Averages and standard errors of at least three independent measurements are shown.

2004). Aire and CCL21 were detectable in mTEC clusters of TCRα-deficient or ZAP70-deficient mice, unlike in the thymus of RelB-deficient (*Relb*$^{-/-}$) mice where mTEC development was defective (Figure 1A). Quantitative mRNA analysis showed that mTECs isolated from TCRα-deficient or ZAP70-deficient mice indeed expressed Aire and CCL21 (Figure 1D). The generation of CD80-expressing mature mTECs was also detectable in TCRα-deficient or ZAP70-deficient mice (data not shown). The expression of Aire-dependent tissue-restricted genes, such as insulin 2 and salivary protein 1, was detectable in mTECs of TCRα-deficient or ZAP70-deficient mice, indicating that mTECs in these mice were capable of Aire-dependent promiscuous gene expression (Figure 1D). cTECs from TCRα-deficient or ZAP70-deficient mice expressed cathepsin L and β5t (Figure 1D), the molecules essential for thymocyte development in the cortex (Honey et al., 2002; Murata et al., 2007). These results indicate that mTECs and cTECs generated without positive selection express molecules that represent their functional maturity.

Small numbers of mTECs including Aire-expressing mTECs were detectable even in RAG2-deficient mice that lacked CD4$^+$CD8$^+$ (double-positive, DP) thymocytes (Derbinski et al., 2001; Rossi et al., 2007; also shown in Figure S1 available online), in agreement with the notion that functionally mature mTECs are generated without positive selection. Together, these results indicate that positive selection promotes the increase in the number of mTECs rather than the functional maturation of mTECs and thereby nurtures the formation of thymic medulla.

TNFSF Expressed in Thymocyte Subsets and TNFRSF Expressed in TEC Subsets

In order to explore the molecular mechanisms mediating the increase in mTEC cellularity caused by positive selection, we surveyed oligonucleotide microarray data from our previous study where we compared gene-expression profiles between positively selected TCR-transgenic thymocytes and wild-type thymocytes (Nitta et al., 2006). We noticed that genes encoding tumor necrosis factor superfamily (TNFSF) members, such as lymphotoxin (LT) α, LTβ, and RANKL, were strongly expressed in positively selected TCR-transgenic thymocytes (Table S1). We therefore analyzed the expression of all TNFSF genes in thymocyte subsets fractionated from normal adult thymus according to the expression of CD4 and CD8. As shown in Figure 2A and in agreement with microarray data, LTα, TNFα, LTβ, OX40L, CD40L, FasL, CD30L, and RANKL were expressed at significantly ($p < 0.05$) higher amounts in CD4$^+$CD8$^-$ and/or CD4$^-$CD8$^+$ (single-positive, SP) thymocytes than in DP thymocytes. LTα, TNFα, LTβ, CD30L, and RANKL expression was high in both CD4$^+$CD8$^-$ and CD4$^-$CD8$^+$ thymocytes, whereas OX40L, CD40L, and FasL expression was high in CD4$^+$CD8$^-$ thymocytes but not in CD4$^-$CD8$^+$ thymocytes. Other TNFSF members showed no significant difference ($p \geq 0.05$) in the expression between DP and SP thymocyte subsets.

We then analyzed the expression of TNF receptor superfamily (TNFRSF) genes in mTECs and cTECs isolated from normal adult thymus. We found that the genes for OX40, CD40, Fas, CD30, 4-1BB, TRAILR2, RANK, OPG, BAFFR, BCMA, RELT, and Eda2r were expressed at significantly ($p < 0.05$) higher amounts in mTECs than in cTECs (Figure 2B). In contrast, the expression of CD27, TWEAKR, GITR, and TNFRH3 was significantly ($p < 0.05$) higher in cTECs than in mTECs. Other TNFRSF members showed no significant difference ($p \geq 0.05$) in the expression between mTECs and cTECs.

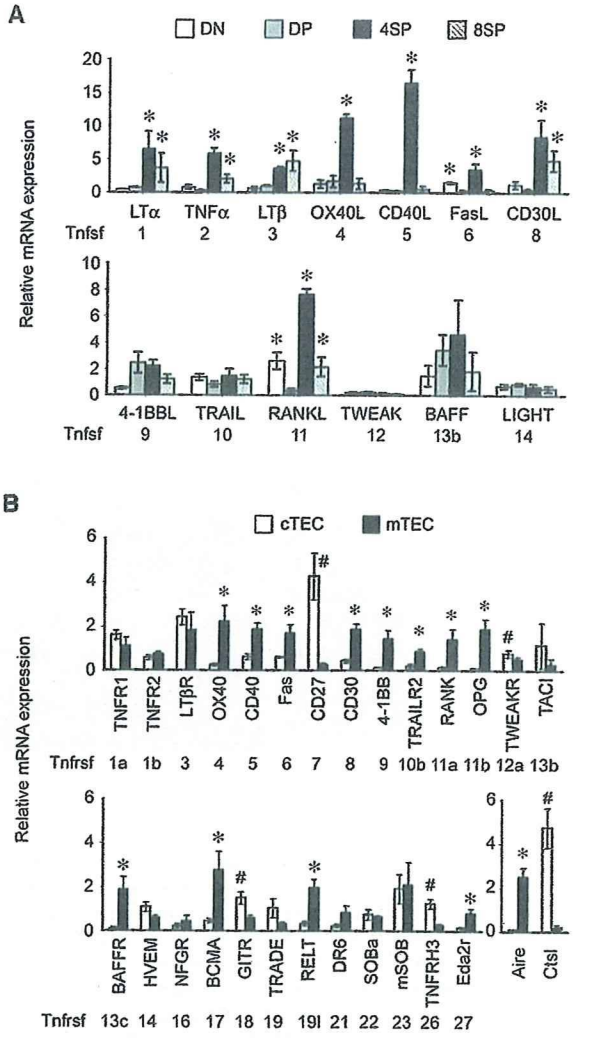

Figure 2. Expression of TNFSF Genes in Thymocytes and TNFRSF Genes in Thymic Epithelial Cells

(A) Quantitative RT-PCR analysis of sorted CD4$^-$CD8$^-$ (DN), CD4$^+$CD8$^+$ (DP), CD4$^+$CD8$^-$ (4SP), and CD4$^-$CD8$^+$ (8SP) thymocytes. mRNA expression of TNFSF genes was normalized to GAPDH mRNA, and those in total thymocytes were arbitrarily set to 1. Bar graphs show means ± standard errors of at least three independent measurements. Asterisks indicate significant ($p < 0.05$) increase compared to the amounts in DP thymocytes. mRNA expression of genes encoding Tnfsf7 (CD27L), Tnfsf13 (APRIL), Tnfsf15 (TL1), and Tnfsf18 (GITRL) was not detectable in total thymocytes or thymocyte subpopulations examined.

(B) Quantitative RT-PCR analysis of sorted CD45$^-$I-A$^+$UEA1$^-$ cTECs and CD45$^-$I-A$^+$UEA1$^+$ mTECs. mRNA expression of TNFRSF genes was normalized to GAPDH mRNA, and those in CD45$^-$ total thymic stromal cells were arbitrarily set to 1. Bar graphs show means ± standard errors of at least three independent measurements. Asterisks indicate significant ($p < 0.05$) increase in mRNAs in mTECs compared to those in cTECs, whereas sharps indicate significant ($p < 0.05$) increase in mRNA amounts in cTECs compared to those in mTECs. mRNA expression of Aire and cathepsin L (Ctsl) indicates successful isolation of mTECs and cTECs, respectively. mRNA expression of Tnfrsf25 (DR3) was not detectable in CD45$^-$ thymus cells, cTECs, or mTECs.

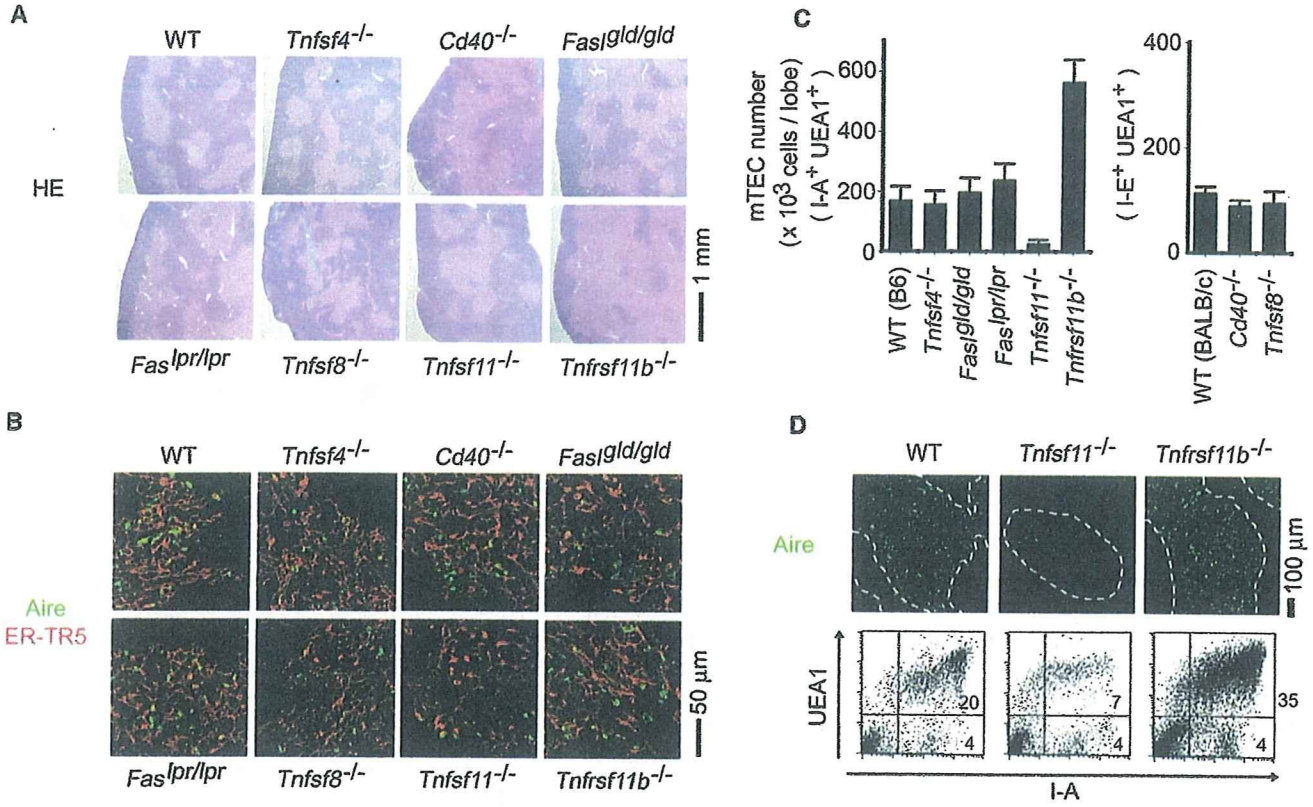

Figure 3. RANKL and OPG Affect Number of mTECs

(A and B) Thymus sections from indicated mice at 3–9 weeks old were analyzed by HE staining (A) and two-color immunostaining with antibody specific for Aire (green) and ER-TR5 (red) (B). B6 mice were used as wild-type (WT) control.

(C) Numbers of mTECs per thymus lobe were calculated by flow cytometry analysis of $CD45^-I\text{-}A^{b+}UEA1^+$ cells for mice of B6 background (left) and $CD45^-I\text{-}E^{d+}UEA1^+$ cells for mice of BALB/c background (right). Averages and standard errors are shown. B6, n = 6; *Tnfsf4*$^{-/-}$, n = 4; *Fasl*$^{gld/gld}$, n = 3; *Fas*$^{lpr/lpr}$, n = 3; *Tnfsf11*$^{-/-}$, n = 2; *Tnfrsf11b*$^{-/-}$, n = 3; BALB/c, n = 3; *Cd40*$^{-/-}$, n = 3; *Tnfsf8*$^{-/-}$, n = 3.

(D) Representative low-magnification images of Aire immunostaining in medullary region identified by ER-TR5 staining and marked by dotted lines, indicating that Aire-expressing cells are present in all three groups but are fewer and more detectable in the thymus of *Tnfsf11*$^{-/-}$ and *Tnfrsf11b*$^{-/-}$ mice, respectively, than in B6 wild-type (WT) mice. Representative two-color flow cytometry profiles for I-A and UEA1 of $CD45^-$ nonleukocytes of indicated mice are also shown. Numbers in quadrants indicate frequency of cells in boxes.

Consequently, we found that in the following five TNFSF ligand-receptor combinations, namely, between OX40L and OX40, between CD40L and CD40, between FasL and Fas, between CD30L and CD30, and among RANKL, RANK (signaling receptor for RANKL), and OPG (nonsignaling soluble decoy receptor for RANKL; Theill et al., 2002), ligands were more strongly expressed in SP thymocytes than in DP thymocytes and receptors were more strongly expressed in mTECs than in cTECs.

RANKL and OPG Influence mTEC Cellularity

We next examined mTEC development and medulla formation in mice deficient for one of the five TNFSF ligand-receptor combinations. We found that the deficiency of OX40L (*Tnfsf4*$^{-/-}$), CD40 (*Cd40*$^{-/-}$), FasL (*Fasl*$^{gld/gld}$), Fas (*Fas*$^{lpr/lpr}$), or CD30L (*Tnfsf8*$^{-/-}$) did not significantly ($p \geq 0.05$) affect the number of mTECs, the generation of Aire-expressing mTECs, or medulla formation (Figures 3A–3C). However, mice deficient for RANKL (*Tnfsf11*$^{-/-}$) exhibited a significant ($p < 0.05$) reduction in the number of mTECs (Figure 3C). In the thymus of RANKL-deficient mice, the number of Aire-expressing mTECs was also decreased as shown by immunohistological analysis (Figure 3D). Nonetheless, the development of Aire-expressing mTECs and the formation of thymic medulla were detectable in the thymus of RANKL-deficient mice (Figures 3A–3C). In contrast, mice deficient for OPG (*Tnfrsf11b*$^{-/-}$), a soluble decoy receptor for RANKL (Theill et al., 2002) and the receptor more strongly expressed in mTECs than in cTECs (Figure 2B), developed a significantly ($p < 0.05$) large number of mTECs and exhibited large thymic medulla with many Aire-expressing mTECs (Figures 3A–3D).

These results indicate that among TNFSF members that are more strongly expressed in SP thymocytes than in DP thymocytes, RANKL plays a major role in increasing the number of mTECs, and its decoy receptor, OPG, regulates mTEC cellularity and medulla formation.

RANKL Is Produced by Positively Selected Thymocytes

The expression of RANKL in normal adult mice was detectable in bulk $CD4^+CD8^-$ and $CD4^-CD8^+$ SP thymocytes but not DP thymocytes, as determined by quantitative mRNA analysis (Figures 2A and 4A). RANKL expression was detectable in $CD69^{hi}$ semimature and $CD69^{lo}$ mature $CD4^+CD8^-$ SP thymocytes isolated from normal B6 mice, both of which expressed $TCR\alpha\beta^{hi}$

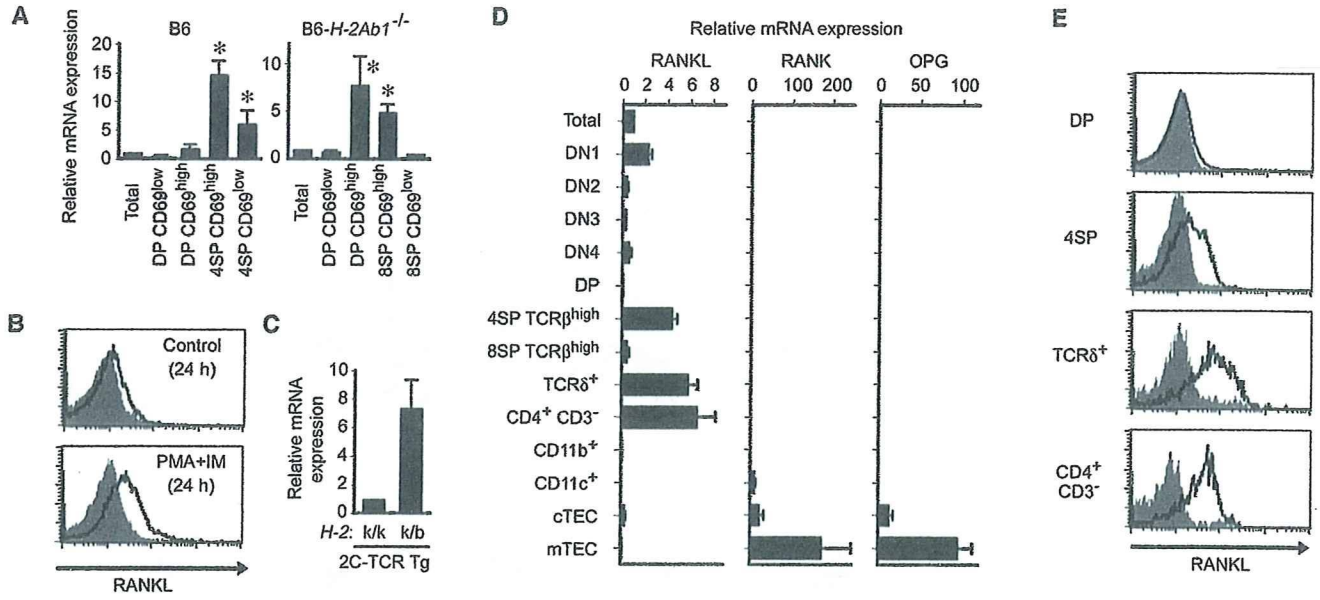

Figure 4. Expression of RANKL, RANK, and OPG in Thymus Cell Subpopulations

(A) mRNA expression of RANKL in total, $CD4^+CD8^+CD69^{lo}$, $CD4^+CD8^+CD69^{hi}$, $CD4^+CD8^-CD69^{hi}$, and $CD4^+CD8^-CD69^{lo}$ thymocytes isolated from 4-week-old B6 mice (n = 4), and total, $CD4^+CD8^+CD69^{lo}$, $CD4^+CD8^+CD69^{hi}$, $CD4^-CD8^+CD69^{hi}$, and $CD4^-CD8^+CD69^{lo}$ thymocytes isolated from MHC class II-deficient 4-week-old B6-*H-2Ab1*$^{-/-}$ mice (n = 3).

(B) Flow cytometry analysis of RANKL expression by TCR-stimulated thymocytes. Thymocytes from 3-week-old MHC class I and class II double-deficient B6-*H-2Ab1*$^{-/-}$*B2m*$^{-/-}$ mice were cultured in the absence or presence of phorbol 12-myristate 13-acetate (PMA, 0.2 ng/ml) and ionomycin (0.2 μg/ml) for 24 hr. RANKL staining profiles (solid lines) and control staining profiles (shaded lines) are shown. Representative profiles of three independent experiments are shown.

(C) mRNA expression of RANKL in $CD4^+CD8^+$ thymocytes isolated from positively selecting *H-2*$^{k/b}$ 2C-TCR-transgenic mice and null selecting *H-2*$^{k/k}$ 2C-TCR-transgenic mice (n = 3).

(D) mRNA expression of RANKL, RANK, and OPG in indicated thymus cell subpopulations isolated from 4- to 5-week-old B6 mice. DN1, DN2, DN3, and DN4 represent $CD4^-CD8^-CD25^-CD44^+$, $CD4^-CD8^-CD25^+CD44^+$, $CD4^-CD8^-CD25^+CD44^-$, and $CD4^-CD8^-CD25^-CD44^-$ thymocyte subpopulations. $CD4^+CD3^-CD8^-B220^-CD11c^-$ thymocyte subpopulation was used as $CD4^+CD3^-$ cells (Rossi et al., 2007). $CD45^-I\text{-}A^+UEA1^-$ cTECs and $CD45^-I\text{-}A^+UEA1^+$ mTECs were used. mRNA expression in total thymus cells are normalized to 1. Averages and standard errors (n = 3) are shown. Note that $CD4^+CD8^-TCR\beta^{hi}$ cells, $TCR\delta^+$ cells, and $CD4^+CD3^-$ cells are the three major cells that express RANKL mRNA in the thymus. RANKL expression detectable in DN1 ($CD44^+CD25^-CD4^-CD8^-$) cells may be due to $TCR\gamma\delta^+$ cells that are contained in DN1 population.

(E) Cell-surface RANKL detection (solid lines) and control staining (shaded lines) were examined in indicated subpopulations of 5-week-old B6 thymocytes incubated for 16 hr without stimulation. Representative profiles of three independent experiments are shown.

(Figure 4A). RANKL was also detectable in $CD69^{hi}$ semimature $CD4^-CD8^+$ SP thymocytes, rather than $CD69^{lo}$ mature $CD4^-CD8^+$ SP thymocytes, isolated from MHC class II-deficient mice (Figure 4A), indicating that RANKL is expressed in semimature thymocytes that are destined to become either $CD4^+CD8^-$ or $CD4^-CD8^+$ SP thymocytes. The $CD69^{hi}$ subpopulation of DP thymocytes, which represent semimature thymocytes that recently received positive-selection-inducing TCR signals (Bendelac et al., 1992), expressed a significantly ($p < 0.05$) higher amount of RANKL than the majority of DP thymocytes, which were $CD69^{lo}$, in MHC class II-deficient mice (Figure 4A). Stimulation of preselected DP thymocytes isolated from MHC class I- and MHC class II-deficient mice (*H-2Ab1*$^{-/-}$*B2m*$^{-/-}$) with plate-bound antibody specific for TCR or with phorbol ester plus ionomycin, which mimics positive-selection-inducing TCR signals (Takahama and Nakauchi, 1996), elevated cell-surface expression of RANKL protein (Figure 4B, data not shown). Indeed, DP thymocytes isolated from positively selecting 2C-TCR-transgenic mice expressed a significantly ($p < 0.05$) higher amount of RANKL than did DP thymocytes isolated from null selecting 2C-TCR-transgenic mice (Figure 4C). These results indicate that RANKL is produced in semimature thymocytes that recently received positive-selection-inducing TCR signals. These results also suggest that the amount and kinetics of RANKL expression may be unequal between cells destined to become $CD4^+CD8^-$ T lymphocytes and those destined to become $CD4^-CD8^+$ T lymphocytes.

$TCR\gamma\delta^+$ Cells or Id2-Dependent LTi Cells Are Dispensable for Medulla Formation in Adult Mice

To address whether cells other than positively selected thymocytes might produce RANKL in the thymus, we examined the expression of RANKL as well as its receptors, RANK and OPG, in various cell subpopulations isolated from adult thymus (Figure 4D). We found that in addition to positively selected SP thymocytes, RANKL expression in the thymus was highly detectable in $TCR\gamma\delta^+$ cells and $CD4^+CD3^-$ LTi cells, as assessed by quantitative mRNA analysis (Figure 4D) and by cell-surface protein analysis (Figure 4E). The detection of RANKL in SP thymocytes was specific, as indicated by the fact that no signals were detected in SP thymocytes isolated from RANKL-deficient mice (Figure S2). RANKL expression was detectable in CD4SP thymocytes from embryonic day 18.5 (E18.5) mice and 1-day-old newborn mice (Figure S3), suggesting that newly generated

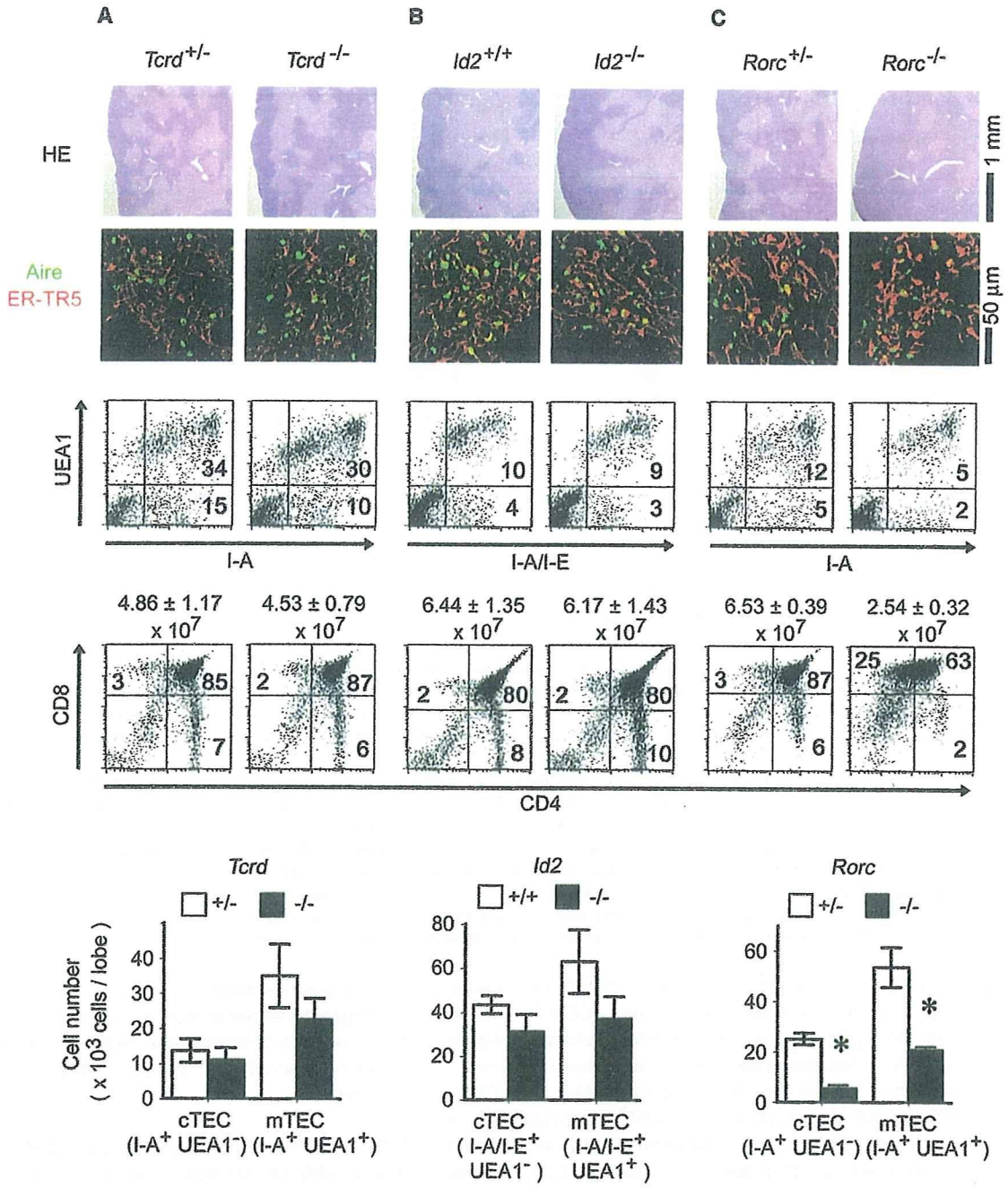

Figure 5. Thymic Epithelial Cells in TCRδ-, Id2-, or RORγt-Deficient Mice

Thymuses from age- and genetic background-matched *Tcrd*$^{+/-}$ and *Tcrd*$^{-/-}$ mice (B6 background [A]), *Id2*$^{+/+}$ and *Id2*$^{-/-}$ mice (ICR background [B]), or *Rorc*$^{+/-}$ and *Rorc*$^{-/-}$ mice (B6 background [C]) were subjected to section analysis and flow cytometry analysis as indicated. A monoclonal antibody specific for both I-A and I-E (clone M5/114) was used to detect class II MHC molecules in mice of ICR background. Averages and standard errors of thymocyte numbers per thymus lobe are also shown. Bar graphs show averages and standard errors of the numbers of CD45$^-$I-A$^+$UEA1$^-$ cTECs and CD45$^-$I-A$^+$UEA1$^+$ mTECs in indicated mice. *Tcrd*$^{+/-}$, n = 4; *Tcrd*$^{-/-}$, n = 5; *Id2*$^{+/+}$, n = 5; *Id2*$^{-/-}$, n = 6; *Rorc*$^{+/-}$, n = 3; *Rorc*$^{-/-}$, n = 3. Asterisks indicate significant difference ($p < 0.01$).

SP thymocytes can be the source of RANKL in the thymus. The detection of RANKL in CD4$^+$CD3$^-$ LTi cells of adult thymus was in agreement with previously reported results (Rossi et al., 2007). On the other hand, among thymic cell subpopulations examined, RANK and OPG were most prominently and almost exclusively detected in mTECs (Figure 4D).

In contrast to mice deficient for positive selection (Figure 1), we found no significant ($p \geq 0.05$) impairment in the number of mTECs or the development of thymic medulla containing Aire-expressing mTECs in adult mice lacking TCRδ (*Tcrd*$^{-/-}$) (Figure 5A) or adult mice deficient for Id2 (*Id2*$^{-/-}$) (Figure 5B; Figure S4), in which LTi cells in embryonic intestine are barely

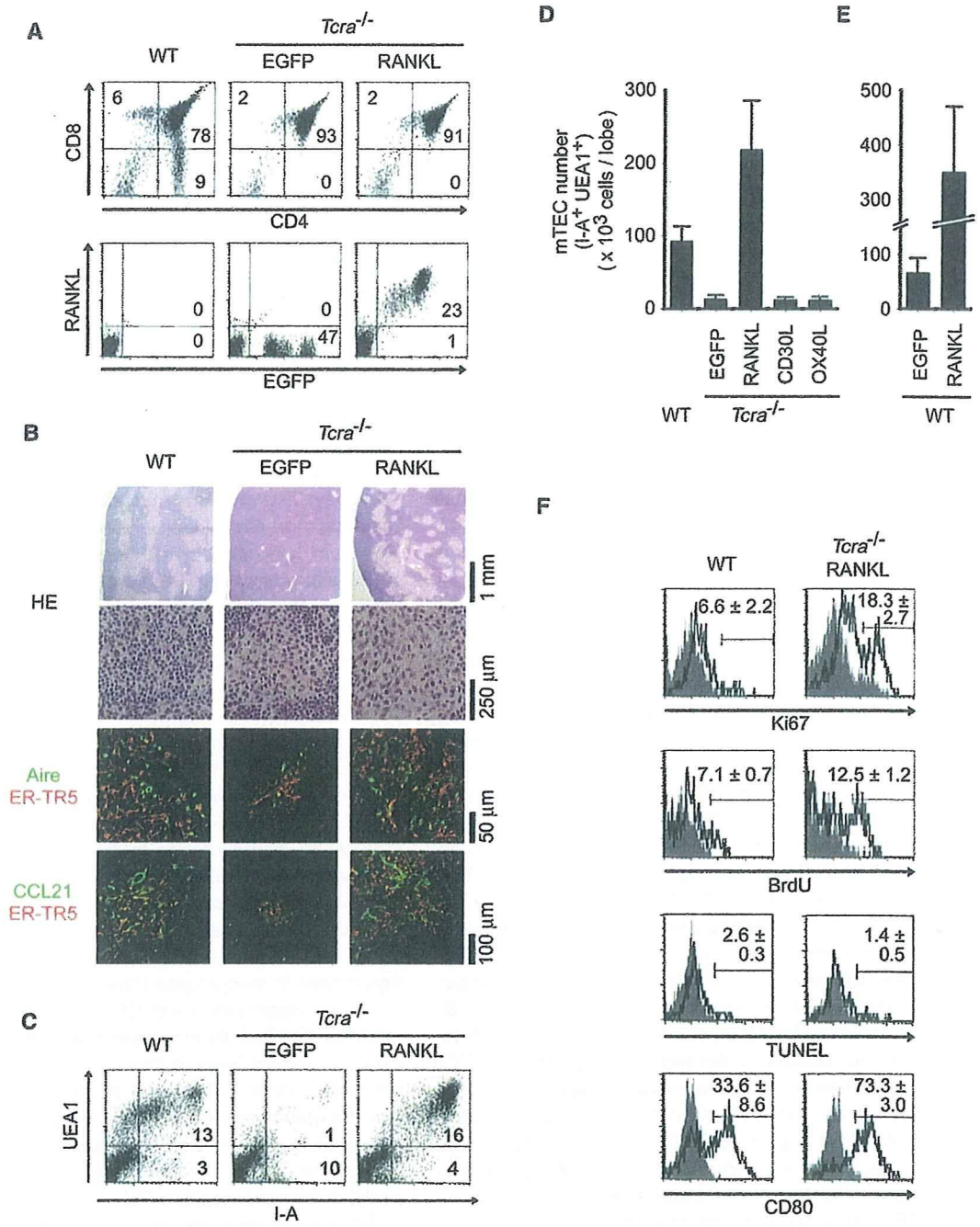

Figure 6. RANKL Expression Restores Medulla Formation without Positive Selection

Sca1$^+$ bone marrow cells from *Tcra*$^{-/-}$ mice were infected with retrovirus expressing RANKL along with EGFP or EGFP alone, and transplanted into lethally irradiated *Tcra*$^{-/-}$ mice. Mice were analyzed 4–5 weeks after transplantation. Frequencies of EGFP$^+$ cells in thymocytes ranged from 23% to 73%.

(A) Flow cytometry profiles of ungated thymocytes from adult B6 mice (WT), *Tcra*$^{-/-}$ mice expressing EGFP alone, or *Tcra*$^{-/-}$ mice expressing RANKL along with EGFP. Numbers indicate frequency of cells within indicated areas.

(B) Thymus section analysis. High-magnification HE-stained images show that thymic medullary areas generated in RANKL-expressing *Tcra*$^{-/-}$ mice are devoid of lymphoid cells, and this finding was supported by the failure to detect CD4- or CD8-expressing cells in those areas (not shown).

(C) Representative results of flow cytometry analysis for I-A$^+$UEA1$^+$ mTECs in CD45$^-$ nonleukocytes.

(D) Numbers (averages and standard errors) of CD45$^-$I-A$^+$UEA1$^+$ mTECs per thymus lobe in B6 mice (WT) or *Tcra*$^{-/-}$ mice reconstituted with *Tcra*$^{-/-}$ bone marrow cells that retrovirally expressed EGFP alone or EGFP along with RANKL, CD30L, or OX40L. WT, n = 6; EGFP, n = 4; RANKL, n = 3; CD30L, n = 3; OX40L, n = 3.

(E) Numbers (averages and standard errors) of CD45$^-$I-A$^+$UEA1$^+$ mTECs per thymus lobe in B6 mice (WT) reconstituted with bone marrow cells that expressed EGFP alone or EGFP along with RANKL, indicating that retroviral expression of RANKL increases the number of mTECs even in normal mice. EGFP, n = 4; RANKL, n = 3.

detectable (Yokota et al., 1999), indicating that unlike positively selected thymocytes, TCRγδ$^+$ cells and Id2-dependent LTi cells are dispensable for mTEC development and medulla formation in adult mice. However, the number of mTECs appeared slightly, although not significantly ($p \geq 0.05$), reduced in TCRδ-deficient mice or Id2-deficient mice (Figures 5A and 5B), suggesting that TCRγδ$^+$ cells and Id2-dependent LTi cells may partially contribute to the optimal cellularity of mTECs.

Similar to Id2-deficient mice, Aire-expressing mTECs were detectable in RORγt-deficient (*Rorc*$^{-/-}$) mice (Figure 5C) lacking LTi cells (Eberl et al., 2004). Unlike Id2-deficient mice, however, RORγt-deficient mice exhibited reduced number of mTECs and small medulla (Figure 5C). The deficiency in RORγt causes not only loss of LTi cells but also reduction in the numbers of DP and SP thymocytes because of reduced survival of DP thymocytes (Sun et al., 2000; also shown in Figure 5C). Accordingly, the number of cTECs was significantly ($p < 0.01$) reduced in RORγt-deficient mice, unlike Id2-deficient mice (Figures 5B and 5C). Thus, the reduced number of mTECs in RORγt-deficient mice may be due to the reduced number of DP and SP thymocytes, including positively selected thymocytes, rather than the loss of LTi cells.

RANKL Neutralization Perturbs mTEC Cellularity

The above-mentioned results suggest that RANKL produced by positively selected thymocytes plays a major role in expanding mTEC cellularity to form thymic medulla. We then examined whether RANKL expressed by developing thymocytes is essential for medulla formation in normal adult mice. To do so, normal B6 mice were reconstituted with B6 bone marrow hematopoietic progenitor cells that were infected with a retrovirus that expressed a soluble fusion protein of RANK and human immunoglobulin Fc portion (RANK-Fc) along with enhanced green fluorescence protein (EGFP). RANK-Fc fusion protein used in this study specifically binds to RANKL (Figure S5A) and neutralizes RANKL-mediated signals (Hsu et al., 1999). Thymocyte development, including the generation of SP thymocytes, was apparently not affected in RANK-Fc-expressing mice (Figure S5B). However, the number of mTECs was significantly ($p < 0.05$) reduced and thymic medulla containing Aire-expressing mTECs became underrepresented in B6 mice expressing RANK-Fc (Figures S5C–S5E). In contrast, RANK-Fc expression did not affect the number of cTECs (Figure S5E). These results indicate that in vivo blockade of RANKL perturbs mTEC cellularity and medulla formation in normal mice and that RANKL is essential for increasing mTEC cellularity and forming thymic medulla.

RANKL Expression Restores Thymic Medulla without Positive Selection

Finally, we addressed whether RANKL expression in developing thymocytes might be sufficient for increasing mTEC cellularity and forming thymic medulla even without positive selection. To do so, bone marrow hematopoietic progenitor cells from TCRα-deficient (*Tcra*$^{-/-}$) mice were infected with a retrovirus that expressed RANKL along with EGFP and were transferred into TCRα-deficient mice. In these mice, positive-selection-mediated generation of mature SP thymocytes remained defective because of the lack of TCR expression by DP thymocytes, whereas RANKL expression was detectable in the majority of EGFP$^+$ thymocytes (Figure 6A). We found that the number of mTECs was significantly ($p < 0.01$) restored and thymic medulla containing Aire-expressing and CCL21-expressing mTECs was obviously formed in RANKL-expressing TCRα-deficient mice but not in control EGFP-expressing TCRα-deficient mice (Figures 6B–6D). Thymic medulla formed in RANKL-expressing TCRα-deficient mice was not colonized with thymocytes because of the lack of positive selection (Figure 6B). Unlike RANKL expression, the expression of CD30L or OX40L did not restore the number of mTECs (Figure 6D). These results indicate that forced RANKL expression was sufficient in vivo for increasing mTEC cellularity and forming thymic medulla even without positive selection.

In order to better understand how RANKL expression increases mTEC cellularity, we measured Ki67 expression in proliferating cells, BrdU incorporation in DNA synthesizing cells, and TUNEL in dying cells, in mTECs of TCRα-deficient mice reconstituted with retrovirally RANKL-expressing TCRα-deficient bone marrow cells. As shown in Figure 6F, RANKL expression elevated the frequency of Ki67-expressing cells and BrdU-incorporated cells in mTECs compared to those in mTECs isolated from wild-type mice. The frequency of TUNEL$^+$ cells was only slightly reduced by RANKL expression (Figure 6F). RANKL expression also elevated the frequency of CD80-expressing mature cells in mTECs (Figure 6F). These results indicate that RANKL expression in bone-marrow-derived cells causes elevated proliferation of mTECs without positive selection, suggesting the possibility that RANKL contributes to medulla formation by promoting the proliferation of mTECs.

We finally addressed whether RANKL produced by SP thymocytes could directly promote the increase in mTEC cellularity. To do so, fetal thymus stromal cells were cultured with isolated SP thymocytes in reaggregated thymus organ culture. As shown in Figure 7, reaggregation with CD4SP thymocytes but not DP thymocytes significantly increased the number of mTECs but not cTECs in culture (Figures 7A and 7B). The number of CD80-expressing mature mTECs and the mRNA amounts of Aire and Aire-dependent tissue-restricted self-antigens (insulin 2 and salivary protein 1) were also increased by the addition of CD4SP thymocytes but not DP thymocytes (Figures 7B and 7C). Importantly, these increases in mTEC cellularity and the expression of mTEC-associated molecules were significantly ($p < 0.05$) diminished by the addition of RANK-Fc (Figure 7), which competitively antagonized RANKL (Figure S5). These results indicate that SP thymocytes are sufficient and RANKL is essential for fostering mTECs.

DISCUSSION

The present results show that positive selection promotes the increase in the number of mTECs and thereby fosters the

(F) Ki67 expression, BrdU incorporation, TUNEL, and CD80 expression were detected in CD45$^-$I-A$^+$UEA1$^+$ mTECs. BrdU (2 mg) was intravenously administered 24 hr before analysis. Shaded profiles indicate control staining. Numbers indicate averages and standard errors (from at least three independent measurements) of frequency of cells within indicated areas.

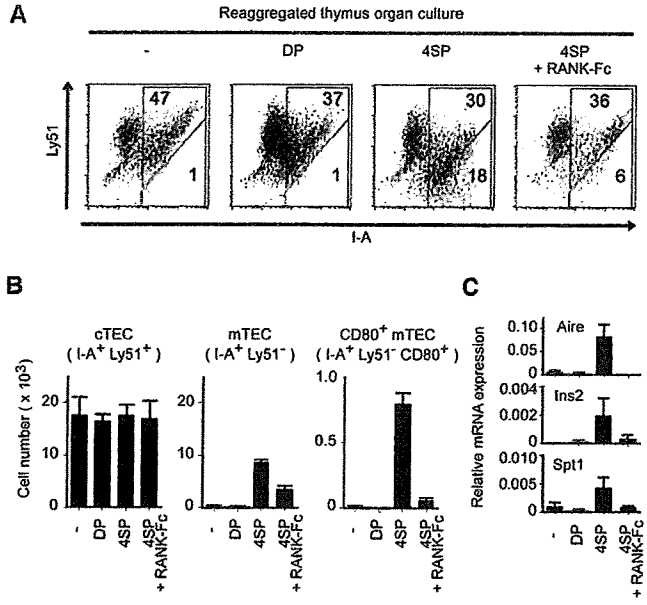

Figure 7. RANKL Produced by SP Thymocytes Promotes mTEC Cellularity in Reaggregated Thymus Organ Culture

dGuo-treated fetal thymic stromal cells (2.5×10^5) were reaggregated with equal numbers of either DP thymocytes from *Tcra*$^{-/-}$ mice or CD4SP thymocytes from B6 mice and organ cultured for 5 days. Where indicated, organ cultures included 5 μg/ml of RANK-Fc fusion protein. Cells were analyzed by flow cytometry (A and B) or quantitative RT-PCR (C).

(A) Representative two-color flow cytometry profiles for I-A and Ly51 of CD45$^-$ nonleukocytes. Numbers indicate frequency of cells within indicated areas.

(B) Numbers of indicated TEC populations per reaggregated thymus organ culture. Averages and standard errors (n = 4–5) are shown.

(C) Quantitative RT-PCR analysis of indicated genes. mRNA expression was normalized to GAPDH mRNA, and those in CD45$^-$I-A$^+$UEA1$^+$ mTECs isolated from adult thymus were arbitrarily set to 1. Averages and standard errors of 4–5 independent measurements are shown.

formation of thymic medulla containing Aire-expressing mTECs. In the absence of positive selection, not only is T lymphocyte development arrested at the DP thymocyte stage, but medulla formation is impaired as well. Through gene-expression analysis of positively selected thymocytes and thymic epithelial cells, we found that RANKL is produced by positively selected thymocytes and that RANKL receptors, RANK and OPG, are expressed by mTECs rather than by cTECs. Mice deficient for RANKL showed a reduction in the number of mTECs, whereas mice deficient for OPG showed a large number of mTECs and a large thymic medulla. Although RANKL expression in the thymus is also detectable in TCR$\gamma\delta^+$ cells and CD4$^+$CD3$^-$ LTi cells, these cells appear dispensable for mTEC generation and medulla formation. The blockade of RANKL perturbs mTEC cellularity in normal mice, whereas forced expression of RANKL restores mTEC cellularity and medulla formation in mice lacking positive selection. These results indicate that RANKL produced by positively selected thymocytes plays a major role in the increase in the number of mTECs and the formation of thymic medulla that contains Aire-expressing mTECs.

Several studies have shown that positively selected thymocytes produce signals crucial for thymic medulla formation (Shores et al., 1991; Surh et al., 1992; Naspetti et al., 1997; Nasreen et al., 2003). However, it was unclear whether positive selection regulates the genesis or increase in number of functionally competent mTECs. The present results show that the lack of positive selection reduces the number of mTECs, whereas small numbers of mTECs detectable in mice lacking positive selection contain Aire-expressing cells and CCL21-expressing cells. Aire and CCL21 are two major molecules that are vital to the execution of thymic medulla function to induce central tolerance, by displaying a diverse set of tissue-restricted genes (Derbinski et al., 2001) and by attracting CCR7-expressing positively selected cortical thymocytes toward the medulla (Ueno et al., 2004), respectively. Indeed, our results show that mTECs generated without positive selection exhibit a gene-expression profile that is characteristic of promiscuous gene expression. These results support the notion that positive selection affects the formation of thymic medulla by promoting the increase in the number of functionally competent mTECs rather than by inducing the functional maturation of mTECs. These results also suggest that thymic medulla formation consists of two sequential processes: initial maturation of mTECs independent of positive selection and subsequent increase in the number of mTECs, which is dependent on positively selected thymocytes. Our results showing that RANKL expression in bone-marrow-derived cells causes elevated proliferation of mTECs without positive selection suggest that RANKL contributes to enhancing mTEC proliferation.

Through microarray data search for genes that are highly expressed upon positive selection, we found that the expression of eight TNFSF genes encoding LTα, TNFα, LTβ, OX40L, CD40L, FasL, CD30L, and RANKL was elevated during the differentiation of DP thymocytes into SP thymocytes. Subsequent survey of genes that are more strongly expressed in mTECs than in cTECs showed that five TNFSF ligand-receptor combinations, namely, between OX40L and OX40, between CD40L and CD40, between FasL and Fas, between CD30L and CD30, and among RANKL, RANK, and OPG, represent combinations in which the ligands are more strongly expressed in SP thymocytes than in DP thymocytes and the receptors are more strongly expressed in mTECs than in cTECs. Analysis of mTEC number and medulla formation in mice deficient for one of these molecules showed that the interaction among RANKL, RANK, and OPG critically regulates the increase in the number of mTECs that leads to medulla formation. Even though the present results obtained via mice deficient for OX40L, CD40, Fas, FasL, or CD30L did not reveal the role of these molecules in regulating mTEC cellularity or medulla formation, our study does not exclude the possibility that these molecules may also be involved in regulating medulla formation. Previous studies of the roles of LTβR (Boehm et al., 2003; Chin et al., 2003; Venanzi et al., 2007) and CD40L (Dunn et al., 1997; Clegg et al., 1997) in medulla development suggest the role of additional TNFSF ligands other than RANKL in generating normal thymic medulla. Indeed, our results indicate that the number of mTECs in RANKL-deficient mice is larger than that in TCRα-deficient or ZAP70-deficient mice, suggesting that the increase in mTEC cellularity caused by positively selected thymocytes may be additionally regulated by signals other than RANKL.

Accordingly, Akiyama et al. (2008) in this issue of *Immunity* found the cooperative roles of CD40L and RANKL in postnatal

medulla formation, by showing that mTEC development is more severely affected in mice doubly deficient for RANKL and CD40 than in RANKL-deficient mice. In CD40-deficient mice, the absolute number of mTECs is not reduced, yet the frequency of class II MHC^{lo} subsets of mTECs is reduced (Akiyama et al., 2008). Thus, the defect in mTECs is much milder in CD40-deficient mice than in RANKL-deficient mice. The reduced frequency of class II MHC^{lo} subsets of mTECs was also reported in CD40L-deficient mice (Gray et al., 2006). We think that RANKL and CD40 at least partially compensate each other but unequally contribute to mTEC development, in which RANKL and CD40L play major and minor roles, respectively.

The intrathymic expression profiles of CD40L and CD40 are somewhat similar to those of RANKL and RANK, respectively; CD40L is highly detectable in positively selected thymocytes and CD4$^+$CD3$^-$ cells, whereas CD40 is more strongly detectable in mTECs than in cTECs (Figure S6). However, unlike RANKL, CD40L is not prominently detectable in TCR$\gamma\delta^+$ cells, and unlike RANK, CD40 is also detectable in CD11c$^+$ DC (Figure S6), indicating that the expression profiles of CD40L and CD40 in the thymus are not exactly identical to those of RANKL and RANK. The unequal roles of CD40L and RANKL in the thymus are also evident from our results that, unlike the retroviral expression of RANKL, that of CD40L dramatically reduces thymocyte cellularity and does not elevate mTEC cellularity in bone marrow chimeras (Figure S7). The reduction in thymocyte cellularity was also reported in proximal *Lck* promoter driven CD40L-transgenic thymocytes (Dunn et al., 1997; Clegg et al., 1997). Thus, it appears that CD40L-overexpressing immature thymocytes are inefficient in survival and/or proliferation, further suggesting that RANKL and CD40L play unequal functions in the thymus.

Our results show that the number of mTECs is reduced in the thymus of RANKL-deficient mice, whereas the number of mTECs is increased in the thymus of OPG-deficient mice. The expression of Aire and CCL21 in mTECs is detectable either in RANKL-deficient mice or in OPG-deficient mice. These results suggest that similar to positively selected thymocytes, RANKL regulates the cellularity, rather than the genesis, of functional mTECs. We also found that in vivo blockade of RANKL by a RANK-Fc fusion protein reduces the number of mTECs in normal mice even in the presence of positive selection, whereas forced expression of RANKL in mice deficient for positive selection restores the number of mTEC and medulla formation in vivo. Our results further show that RANKL is expressed in positively selected thymocytes and in TCR-stimulated DP thymocytes. On the other hand, RANKL is produced as a transmembrane cell-surface protein and can be released as a secreted protein from cell surface (Nakashima et al., 2000). Thus, it is conceivable that positive selection of thymocytes in the thymic cortex elevates the expression of RANKL, which acts to increase the number of mTECs even if mTECs may be remotely localized from positively selected thymocytes. Positive selection also induces CCR7 expression by cortical thymocytes, thereby causing the relocation of positively selected thymocytes to the medulla where mTECs produce CCR7 ligands (Ueno et al., 2004; Kurobe et al., 2006). Thus, positive selection signals increase the expression of RANKL and CCR7, thereby directly regulating both the formation of medullary microenvironment where mTECs express RANKL receptors and the migration of positively selected thymocytes toward the medulla where mTECs express CCR7 ligands.

In agreement with our results, Rossi et al. (2007) recently reported that the number of Aire-expressing mTECs was severely reduced in RANK-deficient mice. They also reported that RANKL is produced by CD4$^+$CD3$^-$ LTi cells in the thymus and that the appearance of CD4$^+$CD3$^-$ LTi cells coincides with the appearance of Aire-expressing mTECs during embryogenesis, suggesting that RANKL-expressing CD4$^+$CD3$^-$ LTi cells induce the generation of Aire-expressing mTECs during embryogenesis (Rossi et al., 2007). Our results indeed show that among adult thymocyte subpopulations, CD4$^+$CD3$^-$ LTi cells and TCR$\gamma\delta^+$ cells, in addition to positively selected thymocytes, produce RANKL. However, our results also show that unlike mice lacking positive selection, Id2-deficient mice lacking Id2-dependent LTi cells or TCRδ-deficient mice lacking TCR$\gamma\delta^+$ cells exhibit no impairment in the number of Aire-expressing mTECs and in the formation of thymic medulla in adult mice. Thus, Id2-dependent CD4$^+$CD3$^-$ LTi cells or TCR$\gamma\delta^+$ cells are dispensable for the formation of thymic medulla containing Aire-expressing mTECs in adult thymus. It is possible that LTi cells and/or TCR$\gamma\delta^+$ cells may primarily participate in the generation of mTEC during embryogenesis rather than during postnatal period, and/or LTi cells involved in thymic medulla development may be generated independent of Id2. It is also possible that any cell type expressing RANKL may be sufficient to influence the cellularity of mTECs and that the contribution of positively selected thymocytes may be best highlighted in postnatal thymus, perhaps because SP thymocytes are present in much larger number than other RANKL-expressing cells, such as LTi and TCR$\gamma\delta$ cells.

Our results reveal a role for OPG in thymic medulla formation. OPG is an osteoclastogenesis inhibitory protein that lacks a transmembrane domain and is a secreted decoy receptor for RANKL (Mizuno et al., 1998; Theill et al., 2002). We found that similar to RANK, OPG is strongly expressed in mTECs rather than in cTECs or other cell types within the thymus. We also showed that the deficiency in OPG causes an increase in mTEC number and enlargement of the thymic medulla. These results suggest that OPG-mediated fine-tuning of RANKL availability at mTEC surface crucially regulates RANK-mediated signals in mTECs, perhaps through TRAF6 and NF-κB, to increase the number of mTECs and form thymic medulla.

In conclusion, this study shows that RANKL produced by positively selected thymocytes plays a pivotal role in increasing the number of mTECs and forming thymic medulla that contains Aire-expressing mTECs. The results demonstrate that RANKL represents a major mediator of thymic crosstalk for the formation of medullary microenvironment by positively selected thymocytes. By increasing the number of Aire-expressing mTECs through RANKL, positively selected thymocytes may pave their own way for subsequent developmental regulation in the medulla to establish central tolerance. Indeed, lymphocytes generated without RANKL fail to establish self-tolerance because these cells manifest infiltration and antibody deposition in the liver (Akiyama et al., 2008). Lymphocytes generated without both RANKL and CD40 cause more severe autoimmune phenotypes than those generated without RANKL alone, whereas lymphocytes from CD40-deficient mice exhibit no detectable autoimmunity. Therefore, the severity of autoimmunity among

these mice appears to be well correlated with the defects in mTEC development. Further studies geared toward revealing the molecular mechanisms of TEC development and thymic microenvironment formation are expected to aid in improving our understanding of and controlling diverse and self-tolerant repertoire formation of T lymphocytes.

EXPERIMENTAL PROCEDURES

Mice

C57BL/6 (B6), BALB/c, ICR, B6-*Fasl*$^{gld/gld}$, and B6-*Fas*$^{lpr/lpr}$ mice were purchased from SLC Japan. *Tnfrsf11b*$^{-/-}$ mice (Mizuno et al., 1998) were purchased from CLEA Japan. *Tcra*$^{-/-}$ (Mombaerts et al., 1992), *Zap70*$^{-/-}$ (Negishi et al., 1995), *Rag2*$^{-/-}$ (Shinkai et al., 1993), *Relb*$^{-/-}$ (Burkly et al., 1995), *Tnfsf4*$^{-/-}$ (Murata et al., 2000), *Cd40*$^{-/-}$ (Kawabe et al., 1994), *Tnfsf8*$^{-/-}$ (Blazar et al., 2004), *Tnfsf11*$^{-/-}$ (Kong et al., 1999), *H2-Ab1*$^{-/-}$ (Cosgrove et al., 1991), *B2m*$^{-/-}$ (Koller et al., 1990), *Tcrd*$^{-/-}$ (Itohara et al., 1993), *Id2*$^{-/-}$ (Yokota et al., 1999), and *Rorc*$^{-/-}$ (Sun et al., 2000) mice were previously described. Experiments with mice were performed with consent from the Animal Experimentation Committee of the University of Tokushima.

Retrovirus Infection

PCR-cloned cDNA fragments encoding an open-reading frame of mouse RANKL, OX40L, CD30L, CD40L, or FasL were cloned in the retrovirus vector pMSCV-IRES-EGFP (Nitta et al., 2006). To construct retrovirus vector expressing RANK-Fc, a cDNA fragment encoding the extracellular region of RANK (aa 1–212) was ligated with human IgG1 Fc cDNA (Zettlmeissl et al., 1990) and inserted into pMSCV-IRES-EGFP. Retroviral production and infection were performed as previously described (Ueno et al., 2005). To generate irradiation bone marrow chimeras, bone marrow cells were harvested from donor mice 4 days after intravenous administration of 5-fluorouracil (150 mg/kg). Sca1$^+$ cells were sorted and precultured in growth medium (Iscove's modified Dulbecco's medium containing 20% FCS, L-glutamine, sodium pyruvate, nonessential amino acids, penicillin, streptomycin, 50 ng/ml SCF, 50 ng/ml IL-6, and 10 ng/ml IL-3). 48 hr later, the culture medium was replaced with retroviral supernatants containing 10 μg/ml polybrene, and culture plates were centrifuged at 1000 × g for 90 min at 30°C. Cells were replenished with the growth medium, cultured overnight, and additionally infected at 24 and 48 hr. Cells were intravenously injected into lethally irradiated (9.0 Gy) recipient mice.

Thymus Section Analysis

Frozen thymuses embedded in OCT compound (Sakura Finetek) were sliced into 5 μm-thick sections and stained with hematoxylin and eosin. For multicolor confocal analysis, frozen sections were fixed with acetone and stained with the following antibodies: mTEC-specific ER-TR5 followed by Alexa Fluor 633-conjugated anti-rat IgG antibody (Molecular Probes); anti-Aire antibody (Santa Cruz) followed by FITC- or Alexa Fluor 568-conjugated anti-rabbit IgG antibody (Molecular Probes); biotinylated anti-CCL21 antibody (R&D Systems) or *Ulex europaeus* agglutinin 1 (UEA1) (Vector Laboratories) followed by Alexa Fluor 488- or Alexa Fluor 546-conjugated streptavidin (Molecular Probes). Images were analyzed with TSC SP2 confocal laser-scanning microscope and Leica Confocal software (version 2.6, Leica).

Flow Cytometry Analysis and Sorting of Thymic Stromal Cells

Multicolor flow cytometry analysis and cell sorting were performed with FACSCalibur and FACS-Vantage (BD Biosciences) as described (Ueno et al., 2005). Thymic stromal cells were prepared by digesting thymic fragments with collagenase, dispase, and DNase I (Roche), as described (Gray et al., 2002). For TEC analysis, cells were stained with allophycocyanin-conjugated antibody specific for CD45, FITC-conjugated antibody specific for I-A (or antibody specific for I-E where indicated), and biotinylated UEA1 or biotinylated antibody specific for Ly51 followed by phycoerythrin-conjugated streptavidin. For TEC sorting, CD45$^-$ cells were enriched by depleting CD45$^+$ cells with a magnetic cell sorter (Miltenyi Biotec) prior to FACS cell sorting. Monoclonal antibody specific for RANKL (BioLegend #510003) was used to detect RANKL expression on cell surface. Ki67 expression, bromodeoxyuridine (BrdU) incorporation, and TdT-mediated dUTP nick end labeling (TUNEL) were measured according to the manufacturers' instructions.

Quantitative mRNA Analysis

Total cellular RNA was reverse-transcribed with oligo-dT primer and Superscript III reverse transcriptase (Invitrogen). Real-time RT-PCR was performed with SYBR Premix Ex Taq (TaKaRa) and Light Cycler DX400 (Roche). Amplified signals were confirmed to be single bands over gel electrophoresis, and normalized to GAPDH. Primer sequences are listed in Table S2.

Reaggregated Thymus Organ Culture

Thymic stromal cells isolated from E15.5 fetal thymus lobes that were cultured for 6 days in the presence of 2-deoxyguanosine (dGuo) were reaggregated with equal numbers of either DP thymocytes isolated from adult TCRα-deficient mice or CD4SP thymocytes isolated from adult B6 mice, and organ cultured for 5 days as previously described (Ueno et al., 2005). RANK-Fc fusion protein was produced by transfected 293T cells and purified with protein A-Sepharose (Amersham-Pharmacia).

SUPPLEMENTAL DATA

Supplemental Data include seven figures and two tables and can be found with this article online at http://www.immunity.com/cgi/content/full/29/3/438/DC1/.

ACKNOWLEDGMENTS

We thank H. Kikutani, T. Yasui, K. Sugamura, N. Ishii, D. Littman, S. Fagarasan, E. Podack, I. Negishi, S. Itohara, and M. Nanno for generously providing us the mice used in this study. We thank H. Nakase, T. Ueno, and Q. Cui for critically reading the manuscript. Technical support by S. Nitta is acknowledged. This study was supported by MEXT Grant-in-Aid for Scientific Research on Priority Areas "Immunological Self" and the Mitsubishi Foundation. Y.H. is a visiting graduate student from Nagoya City University Graduate School of Medical Sciences. T.N. is a JSPS Research Fellow.

Received: December 7, 2007
Revised: April 8, 2008
Accepted: June 20, 2008
Published online: September 18, 2008

REFERENCES

Akiyama, T., Maeda, S., Yamane, S., Ogino, K., Kasai, M., Kajiura, F., Matsumoto, M., and Inoue, J. (2005). Dependence of self-tolerance on TRAF6-directed development of thymic stroma. Science *308*, 248–251.

Akiyama, T., Shimo, Y., Yanai, H., Qin, J., Ohshima, D., Maruyama, Y., Asaumi, Y., Kitazawa, J., Takayanagi, H., Penninger, J.M., et al. (2008). The tumor necrosis factor family receptors RANK and CD40 cooperatively establish the thymic medullary microenvironment and self-tolerance. Immunity *29*, this issue, 423–437.

Anderson, M.S., Venanzi, E.S., Klein, L., Chen, Z., Berzins, S.P., Turley, S.J., von Boehmer, H., Bronson, R., Dierich, A., Benoist, C., and Mathis, D. (2002). Projection of an immunological self shadow within the thymus by the aire protein. Science *298*, 1395–1401.

Bendelac, A., Matzinger, P., Seder, R.A., Paul, W.E., and Schwartz, R.H. (1992). Activation events during thymic selection. J. Exp. Med. *175*, 731–742.

Blazar, B.R., Levy, R.B., Mak, T.W., Panoskaltsis-Mortari, A., Muta, H., Jones, M., Roskos, M., Serody, J.S., Yagita, H., Podack, E.R., and Taylor, P.A. (2004). CD30/CD30 ligand (CD153) interaction regulates CD4+ T cell-mediated graft-versus-host disease. J. Immunol. *173*, 2933–2941.

Bleul, C.C., Corbeaux, T., Reuter, A., Fisch, P., Monting, J.S., and Boehm, T. (2006). Formation of a functional thymus initiated by a postnatal epithelial progenitor cell. Nature *441*, 992–996.

Boehm, T., Scheu, S., Pfeffer, K., and Bleul, C.C. (2003). Thymic medullary epithelial cell differentiation, thymocyte emigration, and the control of autoimmunity require lympho-epithelial cross talk via LTβR. J. Exp. Med. *198*, 757–769.

Bonasio, R., Scimone, M.L., Schaerli, P., Grabie, N., Lichtman, A.H., and von Andrian, U.H. (2006). Clonal deletion of thymocytes by circulating dendritic cells homing to the thymus. Nat. Immunol. *7*, 1092–1100.

Burkly, L., Hession, C., Ogata, L., Reilly, C., Marconi, L.A., Olson, D., Tizard, R., Cate, R., and Lo, D. (1995). Expression of relB is required for the development of thymic medulla and dendritic cells. Nature *373*, 531–536.

Chin, R.K., Lo, J.C., Kim, O., Blink, S.E., Christiansen, P.A., Peterson, P., Wang, Y., Ware, C., and Fu, Y.X. (2003). Lymphotoxin pathway directs thymic Aire expression. Nat. Immunol. *4*, 1121–1127.

Clegg, C.H., Rulffes, J.T., Haugen, H.S., Hoggatt, I.H., Aruffo, A., Durham, S.K., Farr, A.G., and Hollenbaugh, D. (1997). Thymus dysfunction and chronic inflammatory disease in gp39 transgenic mice. Int. Immunol. *9*, 1111–1122.

Cosgrove, D., Gray, D., Dierich, A., Kaufman, J., Lemeur, M., Benoist, C., and Mathis, D. (1991). Mice lacking MHC class II molecules. Cell *66*, 1051–1066.

Daniels, M.A., Teixeiro, E., Gill, J., Hausmann, B., Roubaty, D., Holmberg, K., Werlen, G., Hollander, G.A., Gascoigne, N.R., and Palmer, E. (2006). Thymic selection threshold defined by compartmentalization of Ras/MAPK signalling. Nature *444*, 724–729.

Derbinski, J., Schulte, A., Kyewski, B., and Klein, L. (2001). Promiscuous gene expression in medullary thymic epithelial cells mirrors the peripheral self. Nat. Immunol. *2*, 1032–1039.

Dunn, R.J., Luedecker, C.J., Haugen, H.S., Clegg, C.H., and Farr, A.G. (1997). Thymic overexpression of CD40 ligand disrupts normal thymic epithelial organization. J. Histochem. Cytochem. *45*, 129–141.

Eberl, G., Marmon, S., Sunshine, M.J., Rennert, P.D., Choi, Y., and Littman, D.R. (2004). An essential function for the nuclear receptor RORγt in the generation of fetal lymphoid tissue inducer cells. Nat. Immunol. *5*, 64–73.

Finkel, T.H., Cambier, J.C., Kubo, R.T., Born, W.K., Marrack, P., and Kappler, J.W. (1989). The thymus has two functionally distinct populations of immature $\alpha\beta^+$ T cells: one population is deleted by ligation of αβ TCR. Cell *58*, 1047–1054.

Gallegos, A.M., and Bevan, M.J. (2004). Central tolerance to tissue-specific antigens mediated by direct and indirect antigen presentation. J. Exp. Med. *200*, 1039–1049.

Gray, D.H., Chidgey, A.P., and Boyd, R.L. (2002). Analysis of thymic stromal cell populations using flow cytometry. J. Immunol. Methods *260*, 15–28.

Gray, D.H., Seach, N., Ueno, T., Milton, M.K., Liston, A., Lew, A.M., Goodnow, C.C., and Boyd, R.L. (2006). Developmental kinetics, turnover, and stimulatory capacity of thymic epithelial cells. Blood *108*, 3777–3785.

Hamazaki, Y., Fujita, H., Kobayashi, T., Choi, Y., Scott, H.S., Matsumoto, M., and Minato, N. (2007). Medullary thymic epithelial cells expressing Aire represent a unique lineage derived from cells expressing claudin. Nat. Immunol. *8*, 304–311.

Honey, K., Nakagawa, T., Peters, C., and Rudensky, A. (2002). Cathepsin L regulates $CD4^+$ T cell selection independently of its effect on invariant chain: A role in the generation of positively selecting peptide ligands. J. Exp. Med. *195*, 1349–1358.

Hsu, H., Lacey, D.L., Dunstan, C.R., Solovyev, I., Colombero, A., Timms, E., Tan, H.L., Elliott, G., Kelley, M.J., Sarosi, I., et al. (1999). Tumor necrosis factor receptor family member RANK mediates osteoclast differentiation and activation induced by osteoprotegerin ligand. Proc. Natl. Acad. Sci. USA *96*, 3540–3545.

Itohara, S., Mombaerts, P., Lafaille, J., Iacomini, J., Nelson, A., Clarke, A.R., Hooper, M.L., Farr, A., and Tonegawa, S. (1993). T cell receptor δ gene mutant mice: Independent generation of αβ T cells and programmed rearrangements of γδ TCR genes. Cell *72*, 337–348.

Kawabe, T., Naka, T., Yoshida, K., Tanaka, T., Fujiwara, H., Suematsu, S., Yoshida, N., Kishimoto, T., and Kikutani, H. (1994). The immune responses in CD40-deficient mice: Impaired immunoglobulin class switching and germinal center formation. Immunity *1*, 167–178.

Kisielow, P., Teh, H.S., Bluthmann, H., and von Boehmer, H. (1988). Positive selection of antigen-specific T cells in thymus by restricting MHC molecules. Nature *335*, 730–733.

Koller, B.H., Marrack, P., Kappler, J.W., and Smithies, O. (1990). Normal development of mice deficient in β2M, MHC class I proteins, and $CD8^+$ T cells. Science *248*, 1227–1230.

Kong, Y.Y., Yoshida, H., Sarosi, I., Tan, H.L., Timms, E., Capparelli, C., Morony, S., Oliveira-dos-Santos, A.J., Van, G., Itie, A., et al. (1999). OPGL is a key regulator of osteoclastogenesis, lymphocyte development and lymph-node organogenesis. Nature *397*, 315–323.

Kurobe, H., Liu, C., Ueno, T., Saito, F., Ohigashi, I., Seach, N., Arakaki, R., Hayashi, Y., Kitagawa, T., Lipp, M., et al. (2006). CCR7-dependent cortex-to-medulla migration of positively selected thymocytes is essential for establishing central tolerance. Immunity *24*, 165–177.

Kwan, J., and Killeen, N. (2004). CCR7 directs the migration of thymocytes into the thymic medulla. J. Immunol. *172*, 3999–4007.

Mizuno, A., Amizuka, N., Irie, K., Murakami, A., Fujise, N., Kanno, T., Sato, Y., Nakagawa, N., Yasuda, H., Mochizuki, S., et al. (1998). Severe osteoporosis in mice lacking osteoclastogenesis inhibitory factor/osteoprotegerin. Biochem. Biophys. Res. Commun. *247*, 610–615.

Mombaerts, P., Clarke, A.R., Rudnicki, M.A., Iacomini, J., Itohara, S., Lafaille, J.J., Wang, L., Ichikawa, Y., Jaenisch, R., Hooper, M.L., and Tonegawa, S. (1992). Mutations in T-cell antigen receptor genes α and β block thymocyte development at different stages. Nature *360*, 225–231.

Murata, K., Ishii, N., Takano, H., Miura, S., Ndhlovu, L.C., Nose, M., Noda, T., and Sugamura, K. (2000). Impairment of antigen-presenting cell function in mice lacking expression of OX40 ligand. J. Exp. Med. *191*, 365–374.

Murata, S., Sasaki, K., Kishimoto, T., Niwa, S., Hayashi, H., Takahama, Y., and Tanaka, K. (2007). Regulation of $CD8^+$ T cell development by thymus-specific proteasomes. Science *316*, 1349–1353.

Nakashima, T., Kobayashi, Y., Yamasaki, S., Kawakami, A., Eguchi, K., Sasaki, H., and Sakai, H. (2000). Protein expression and functional difference of membrane-bound and soluble receptor activator of NF-κB ligand: Modulation of the expression by osteotropic factors and cytokines. Biochem. Biophys. Res. Commun. *275*, 768–775.

Naspetti, M., Aurrand-Lions, M., DeKoning, J., Malissen, M., Galland, F., Lo, D., and Naquet, P. (1997). Thymocytes and RelB-dependent medullary epithelial cells provide growth-promoting and organization signals, respectively, to thymic medullary stromal cells. Eur. J. Immunol. *27*, 1392–1397.

Nasreen, M., Ueno, T., Saito, F., and Takahama, Y. (2003). In vivo treatment of class II MHC-deficient mice with anti-TCR antibody restores the generation of circulating CD4 T cells and optimal architecture of thymic medulla. J. Immunol. *171*, 3394–3400.

Negishi, I., Motoyama, N., Nakayama, K., Nakayama, K., Senju, S., Hatakeyama, S., Zhang, Q., Chan, A.C., and Loh, D.Y. (1995). Essential role for ZAP-70 in both positive and negative selection of thymocytes. Nature *376*, 435–438.

Nitta, T., Nasreen, M., Seike, T., Goji, A., Ohigashi, I., Miyazaki, T., Ohta, T., Kanno, M., and Takahama, Y. (2006). IAN family critically regulates survival and development of T lymphocytes. PLoS Biol. *4*, e103.

Philpott, K.L., Viney, J.L., Kay, G., Rastan, S., Gardiner, E.M., Chae, S., Hayday, A.C., and Owen, M.J. (1992). Lymphoid development in mice congenitally lacking T cell receptor αβ-expressing cells. Science *256*, 1448–1452.

Rossi, S.W., Jenkinson, W.E., Anderson, G., and Jenkinson, E.J. (2006). Clonal analysis reveals a common progenitor for thymic cortical and medullary epithelium. Nature *441*, 988–991.

Rossi, S.W., Kim, M.Y., Leibbrandt, A., Parnell, S.M., Jenkinson, W.E., Glanville, S.H., McConnell, F.M., Scott, H.S., Penninger, J.M., Jenkinson, E.J., et al. (2007). RANK signals from $CD4^+3^-$ inducer cells regulate development of Aire-expressing epithelial cells in the thymic medulla. J. Exp. Med. *204*, 1267–1272.

Shinkai, Y., Koyasu, S., Nakayama, K., Murphy, K.M., Loh, D.Y., Reinherz, E.L., and Alt, F.W. (1993). Restoration of T cell development in RAG-2-deficient mice by functional TCR transgenes. Science *259*, 822–825.

Shores, E.W., Van Ewijk, W., and Singer, A. (1991). Disorganization and restoration of thymic medullary epithelial cells in T cell receptor-negative scid mice:

Evidence that receptor-bearing lymphocytes influence maturation of the thymic microenvironment. Eur. J. Immunol. *21*, 1657–1661.

Sun, Z., Unutmaz, D., Zou, Y.R., Sunshine, M.J., Pierani, A., Brenner-Morton, S., Mebius, R.E., and Littman, D.R. (2000). Requirement for RORγ in thymocyte survival and lymphoid organ development. Science *288*, 2369–2373.

Surh, C.D., Ernst, B., and Sprent, J. (1992). Growth of epithelial cells in the thymic medulla is under the control of mature T cells. J. Exp. Med. *176*, 611–616.

Takahama, Y., and Nakauchi, H. (1996). Phorbol ester and calcium ionophore can replace TCR signals that induce positive selection of CD4 T cells. J. Immunol. *157*, 1508–1513.

Theill, L.E., Boyle, W.J., and Penninger, J.M. (2002). RANK-L and RANK: T cells, bone loss, and mammalian evolution. Annu. Rev. Immunol. *20*, 795–823.

Ueno, T., Saito, F., Gray, D.H., Kuse, S., Hieshima, K., Nakano, H., Kakiuchi, T., Lipp, M., Boyd, R.L., and Takahama, Y. (2004). CCR7 signals are essential for cortex-medulla migration of developing thymocytes. J. Exp. Med. *200*, 493–505.

Ueno, T., Liu, C., Nitta, T., and Takahama, Y. (2005). Development of T-lymphocytes in mouse fetal thymus organ culture. Methods Mol. Biol. *290*, 117–133.

van Ewijk, W., Shores, E.W., and Singer, A. (1994). Crosstalk in the mouse thymus. Immunol. Today *15*, 214–217.

Venanzi, E.S., Gray, D.H., Benoist, C., and Mathis, D. (2007). Lymphotoxin pathway and Aire influences on thymic medullary epithelial cells are unconnected. J. Immunol. *179*, 5693–5700.

Yokota, Y., Mansouri, A., Mori, S., Sugawara, S., Adachi, S., Nishikawa, S., and Gruss, P. (1999). Development of peripheral lymphoid organs and natural killer cells depends on the helix-loop-helix inhibitor Id2. Nature *397*, 702–706.

Zettlmeissl, G., Gregersen, J.P., Duport, J.M., Mehdi, S., Reiner, G., and Seed, B. (1990). Expression and characterization of human CD4:immunoglobulin fusion proteins. DNA Cell Biol. *9*, 347–353.

Published November 24, 2008

JEM

ARTICLE

Expression of the retinoblastoma protein RbAp48 in exocrine glands leads to Sjögren's syndrome–like autoimmune exocrinopathy

Naozumi Ishimaru,[1] Rieko Arakaki,[1] Satoko Yoshida,[1] Akiko Yamada,[1] Sumihare Noji,[2] and Yoshio Hayashi[1]

[1]Department of Oral Molecular Pathology, Institute of Health Biosciences, [2]Department of Life Systems, Institute of Technology and Science, The University of Tokushima Graduate School, Tokushima 770-8504, Japan

Although several autoimmune diseases are known to develop in postmenopausal women, the mechanisms by which estrogen deficiency influences autoimmunity remain unclear. Recently, we found that retinoblastoma-associated protein 48 (RbAp48) induces tissue-specific apoptosis in the exocrine glands depending on the level of estrogen deficiency. In this study, we report that transgenic (Tg) expression of RbAp48 resulted in the development of autoimmune exocrinopathy resembling Sjögren's syndrome. $CD4^+$ T cell–mediated autoimmune lesions were aggravated with age, in association with autoantibody productions. Surprisingly, we obtained evidence that salivary and lacrimal epithelial cells can produce interferon-γ (IFN-γ) in addition to interleukin-18, which activates IFN regulatory factor-1 and class II transactivator. Indeed, autoimmune lesions in *Rag2*$^{-/-}$ mice were induced by the adoptive transfer of lymph node T cells from *RbAp48*-Tg mice. These results indicate a novel immunocompetent role of epithelial cells that can produce IFN-γ, resulting in loss of local tolerance before developing gender-based autoimmunity.

CORRESPONDENCE
Yashio Hayashi:
hayashi@dent.tokushima-u.ac.jp

Abbreviations used: CIITA, class II transactivator; cLN, cervical LN; HSG, human salivary gland; IRF, IFN regulatory factor; MSG, mouse salivary gland; NOD, nonobese diabetic; RA, rheumatoid arthritis; RbAp48, retinoblastoma-associated protein 48; SLE, systemic lupus erythematosus; SS, Sjögren's syndrome; Tg, transgenic.

Autoimmune disease is controlled by environments that include gene variants or various cytokines (1, 2). It can increase susceptibility to autoimmunity by affecting the overall reactivity and quality of the cells of the immune system. There is an autoimmune disease specific for certain organs in the body, involving a response to an antigen expressed only in those organs. Antigen/organ specificity is affected by antigen presentation and recognition, antigen expression, and the state and response of the target organs (3, 4), which are maintained by a local immune system termed here "local tolerance."

Many mechanisms protect tissues from autoimmune damage. These include relative isolation from the immune system and inhibition of the function of invading lymphocytes. For example, the eye has barriers to T cell infiltration and produces immunosuppressive cytokines, such as TGF-β (5). Constitutive expression of Fas ligand within the privileged site might also prevent immune-mediated damage by eliminating Fas-expressing T cells (6). Although they have yet to be well demonstrated in spontaneous animal models or human disease, genetic effects at the level of tissue protection are therefore to be expected. Autoimmune organ damage can be mediated by $CD4^+$ T cells, which play a crucial role in the development of autoimmunity (7–9). MHC class II alleles are probably involved in autoimmune disease because different alleles have different abilities to present peptides from target cells to autoreactive $CD4^+$ T cells (10, 11). Certain class II alleles might predispose to autoimmunity by increasing positive selection or decreasing negative selection of autoreactive T cells in the thymus. They might also act by inhibiting selection in the thymus of the regulatory $CD4^+$ T cells that are thought to prevent autoantigen-specific responses. Evidence for the local tolerance hypothesis is provided by the observation that

N. Ishimura and R. Arakaki contributed equally to this paper.
The online version of this article contains supplemental material.

The Rockefeller University Press $30.00
J. Exp. Med. Vol. 205 No. 12 2915-2927
www.jem.org/cgi/doi/10.1084/jem.20080174

Supplemental Material can be found at:
http://jem.rupress.org/content/suppl/2008/11/17/jem.20080174.DC1.html

Published November 24, 2008

autoimmune diseases are often tissue specific and sometimes involve antibodies against a restricted set of antigens, thereby prompting us to accept this most simple explanation for the initiation of autoimmunity. The loss of local tolerance is considered to result from the combined effect of different environmental factors. MHC class II genes are constitutively expressed only on hematopoietic cells involved in antigen presentation (dendritic cells, macrophages, B cells, and cortical thymic epithelial cells), but can be aberrantly induced by inflammatory stimuli on many other cell types (such as endothelial cells, hepatocytes, β cells of the pancreas, and thyrocytes) (12, 13). Although it has been implicated in allograft rejection (14), and subsequently in autoimmunity, it is still unknown whether to initiate autoimmunity class II molecules have to be expressed on professional APCs within secondary lymphoid organs or on nonhematopoietic cells of the target organ itself.

It has been suggested that estrogenic action is responsible for the strong female preponderance of many autoimmune diseases, including systemic lupus erythematosus (SLE), rheumatoid arthritis (RA), and Sjögren's syndrome (SS) (15, 16). Recent evidence suggests that apoptosis plays a key role in the physiology and pathogenesis of various autoimmune diseases, including SS (17–21). We have demonstrated that estrogenic action influences target epithelial cells through Fas-mediated apoptosis in a murine model for SS (21). Recently, we found that tissue-specific apoptosis in the exocrine glands spontaneously occurring in estrogen-deficient mice may contribute to the development of autoimmune exocrinopathy (22). Searching for the role of estrogen deficiency in the development of autoimmunity, we have recently identified retinoblastoma-associated protein 48 (RbAp48) gene specific for estrogen deficiency–dependent apoptosis in the exocrine glands, and transgenic expression of RbAp48 gene induced tissue-specific apoptosis in the exocrine glands (23). In this transgenic mouse model, we propose a possible clear and defined ab initio relationship between aberrant exposure of MHC class II molecules on IFN-γ–producing epithelial cells and disease development (i.e., autoimmune exocrinopathy).

RESULTS

Autoimmune exocrinopathy develops in *RbAp48*-transgenic (Tg) mice

We have generated *RbAp48*-Tg mice where the RbAp48 gene is expressed in the salivary and lacrimal glands using the salivary gland–specific promoter (23). When the histopathology of all organs from those mice were analyzed, we found that autoimmune exocrinopathy resembling SS developed in almost all *RbAp48*-Tg mice at 24 wk of age or more, but not in the WT mice. Lymphocyte infiltration in salivary and lacrimal glands of *RbAp48*-Tg mice becomes more frequent at ~30–50 wk of age (Fig. 1 A), and a significantly higher incidence of inflammatory lesions was found in female Tg mice at all ages (not depicted). Many infiltrating lymphocytes were observed in periductal areas at moderate (score 2) to severe (score 4) degrees, and shown in focal appearance. Representative histopathological features of the inflammatory lesions in lachrymal and salivary (submandibular) glands from *RbAp48*-Tg mice were shown in Fig. 1 B. No inflammatory lesions were observed in other organs of *RbAp48*-Tg mice. A majority of infiltrating cells in salivary and lacrimal glands were Thy1.2$^+$ CD4$^+$ T cells, whereas a minor proportion of B220$^+$ B cells, CD8$^+$ T cells (Fig. 1 C), and CD11b$^+$ cells (unpublished data) was observed. When the function of lacrimal and salivary glands in *RbAp48*-Tg mice was analyzed, the mean volume of tear and saliva secretion from *RbAp48*-Tg mice was significantly lower than that from the WT group at 30 wk of age or more (Fig. 1 D). Regarding the peripheral T cell phenotype of *RbAp48*-Tg mice, T cell activation markers (CD44^{high}, CD62L^{low}, CD45RB^{low}) were up-regulated on CD4$^+$ T cells in cervical LNs (cLNs) from *RbAp48*-Tg mice, compared with those from WT mice (Fig. 2 A). No significant difference was observed in thymic T cells gated on CD4$^+$CD8$^-$ bearing CD69, CD25, and CD62L^{low} between Tg and WT mice (Fig. S1, available at http://www.jem.org/cgi/content/full/jem.20080174/DC1). As for the phenotype of CD4$^+$CD25$^+$Foxp3$^+$ T reg cells, no difference

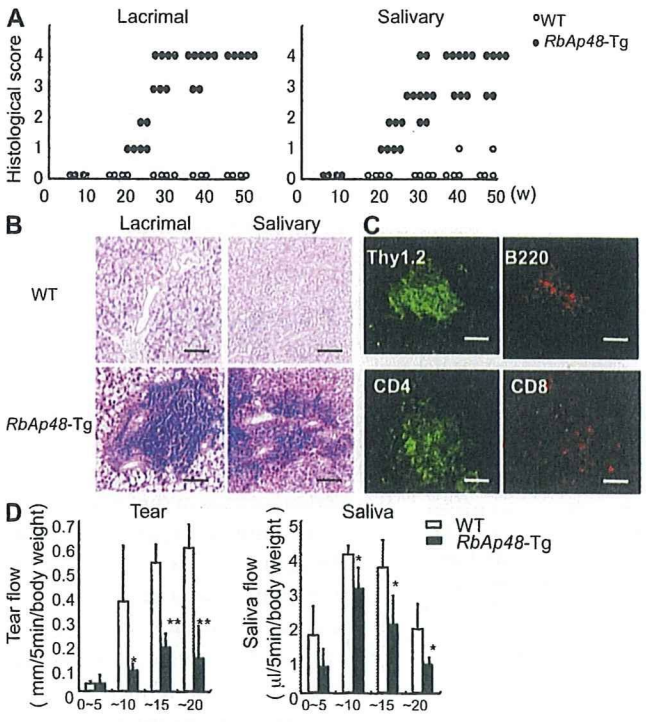

Figure 1. Autoimmune lesions in *RbAp48*-Tg mice. (A) Mean grade of inflammatory lesions in salivary and lacrimal glands from WT and *RbAp48*-Tg mice 10–50 wk of age. (B) Images (H&E staining) are representative of 5–7 mice at 32 wk of age. (C) Lymphocyte populations of the salivary gland lesion from *RbAp48*-Tg mice at 24 wk of age. Thy1.2$^+$, CD4$^+$, CD8$^+$ T cells, or B220$^+$ B cells were detected by immunofluorescence staining with FITC- (green) or PE-conjugated (red) mAbs using the frozen sections. Images are representative of three to five samples from each group. (D) The mean volume of saliva and tear secretion from WT and *RbAp48*-Tg mice at 30 wk of age was measured. Data are means ± SE of five mice. The results are representative of two independent experiments. Bars: (B) 100 μm; (C) 40 μm.

Published November 24, 2008

was detected in thymus, spleen, and cLNs between *RbAp48*-Tg and WT mice (Fig. S2). Moreover, culture supernatants from anti–TCR-β and -CD28 mAb-stimulated cLN T cells obtained from *RbAp48*-Tg mice contained higher levels of IL-2 and IFN-γ, whereas no difference in IL-4 and -10 levels between *RbAp48*-Tg and WT mice was observed by ELISA (Fig. 2 B). Our previous reports identified a 120-kD α-fodrin as an important autoantigen in murine and human SS (24, 25). It is particularly interesting that a higher titer of serum autoantibodies against SS-A (Ro), SS-B (La), and 120-kD α-fodrin was detected in *RbAp48*-Tg mice, compared with that in WT mice by ELISA (Fig. 2 C). This result is consistent with the characteristic flow cytometric finding that showed a significant $CD5^+B220^+$ fraction capable of autoantibody production (26) that appeared in spleen cells from *RbAp48*-Tg mice compared with WT mice (Fig. 2 D). On the other hand, the $CD5^+B220^+$ cells were undetectable in both salivary and lacrimal glands from *RbAp48*-Tg mice (Fig. S3 A). In addition, significantly increased $CD21^{high}IgM^{high}B220^+$ marginal zone B cells were observed in both cervical lymph nodes and spleen from *RbAp48*-Tg mice compared with those from WT mice (Fig. S3). These results may provide a new animal model for autoimmune exocrinopathy resembling SS, which should help us to further understand how autoreactive T cells are developed, and subsequently influence the development of autoimmunity.

Salivary gland epithelial cells function as APCs

It is well known that nonlymphoid cells that express MHC class II molecules provoke autoimmune responses (12, 13). However, it is undetermined whether MHC class II–expressing epithelial cells can function as APCs. We frequently observed MHC class II molecule expression on the exocrine gland cells in *RbAp48*-Tg mice, but not in WT mice (Fig. 3 A). These molecules play a pivotal role in the induction and regulation of immune responses by virtue of their ability to present self-peptides to $CD4^+$ T cells (27). To examine whether salivary epithelial cells could act as APCs, mouse salivary gland (MSG) cells, splenocytes, and splenic $CD11c^+$ DCs from *RbAp48*-Tg mice and WT mice were compared in terms of their capacity to express MHC class II and costimulatory molecules, including CD86, CD80, and ICAM-1, by flow cytometric analysis. Among them, a considerably large proportion of MHC class II^+, $CD86^+$ cells, $CD80^+$ cells, and $ICAM\text{-}1^+$ cells was observed on MSG cells from Tg mice, compared with those from WT mice (Fig. 3 B). MSG cells

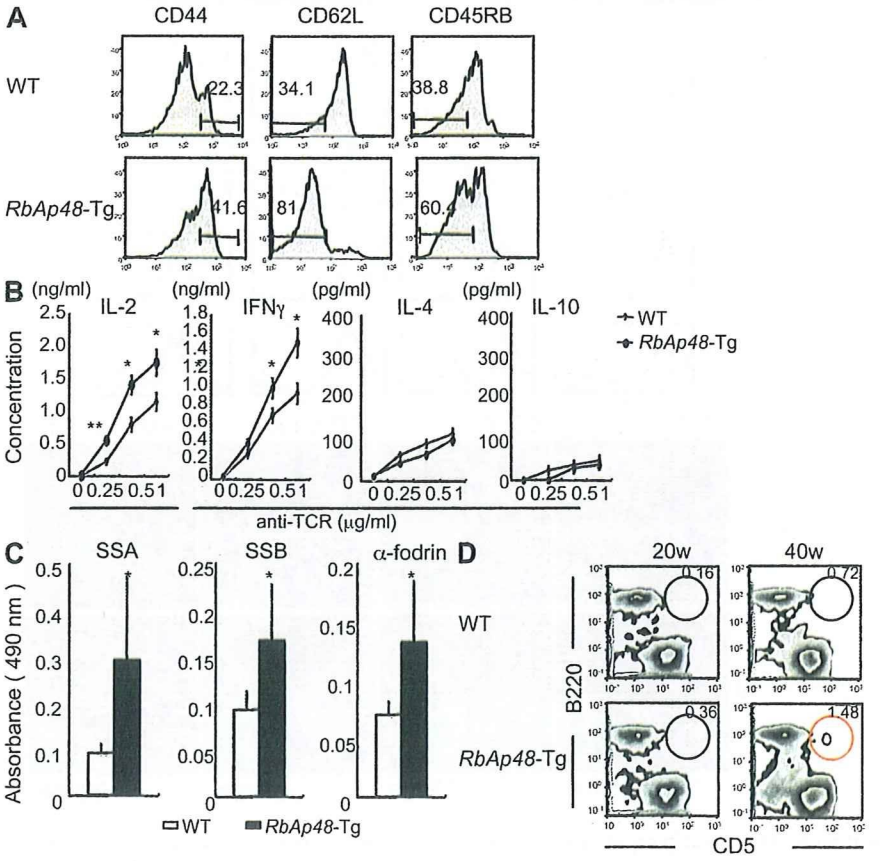

Figure 2. Immune responses in *RbAp48*-Tg mice. (A and B) Activation markers and cytokine production of $CD4^+$ T cells of cLNs from WT and *RbAp48*-Tg mice at 32 wk of age. (C) Autoantibodies of sera from *RbAp48*-Tg mice at 28–32 wk of age. (D) $CD5^+B220^+$ population of spleen from *RbAp48*-Tg and WT mice at 20 and 40 wk of age was analyzed by flow cytometry. Results are representative of means ± SE of five to seven mice in three independent experiments. *, $P < 0.05$; **, $P < 0.005$; WT versus *RbAp48*-Tg mice.

Published November 24, 2008

were enriched by enzymatic treatment and using several antibodies against immune cells, epithelial cells, and magnetic beads, as shown in Fig. S4 A (available at http://www.jem.org/cgi/content/full/jem.20080174/DC1). DCs were undetectable in the purified MSG cell suspension (Fig. S4 B). On the other hand, although the expressions of MHC class II and CD86 on the splenocytes and CD11c$^+$ DCs were higher than those on both MSG cells, the expressions of CD80 and ICAM-1 on the professional APCs were similar or lower than those on the MSG cells (Fig. 3 B). These expressions (MHC class II$^+$, CD86$^+$, CD80$^+$, and ICAM-1$^+$) on salivary epithelial cells from *RbAp48*-Tg mice were also confirmed by confocal analysis (Fig. 3 C). Controls using isotype antibodies for immunostainings were shown in Fig. S4 B. Moreover, to examine whether the peripheral T cells from *RbAp48*-Tg mice can respond to the MSG cells that show phenotypes for the APCs, CFSE-labeled purified CD4$^+$ (10^5) T cells from *RbAp48*-Tg mice were co-cultured with the MSG cells (1 and 2×10^5) from those mice or WT mice. Although CD4$^+$ T cells from B6 mice could not respond to both B6 and *RbAp48*-Tg MSG cells, CD4$^+$ T cells from *RbAp48*-Tg mice were capable of responding to MSG cells from *RbAp48*-Tg mice, but not with those from WT mice, whereas anti–MHC class II antibody inhibits these responses (Fig. 4 A). Furthermore, proliferation assay using [^{3}H]thymidine incorporation demonstrated that purified CD4$^+$ T cells of cLNs from *RbAp48*-Tg mice were more proliferative to the MSG cells from *RbAp48*-Tg mice relative to those from WT mice (Fig. 4 B). Additionally, significantly increased proliferation of the CD4$^+$ T cells to peripheral DCs from *RbAp48*-Tg

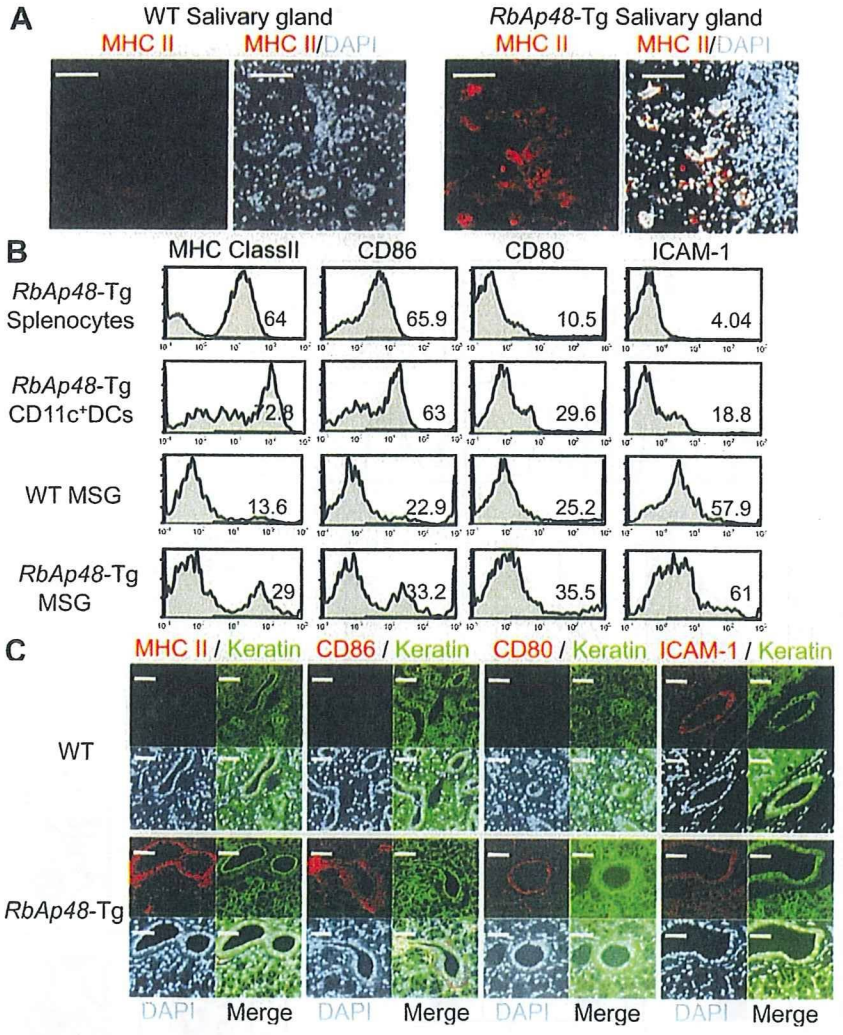

Figure 3. Antigen-presenting function in salivary epithelial cells. (A) MHC class II expression of salivary tissues from WT and *RbAp48*-Tg mice was detected by confocal analysis using anti-MHC class II mAb, Alexa Fluor 568–conjugated anti-rat IgG (red) and DAPI (blue). Images are representative of five to seven mice. (B) APC markers of splenocytes, splenic DCs, and MSG cells from WT and *RbAp48*-Tg mice were analyzed by flow cytometer. Results are representative of three to five mice in two independent experiments. (C) APC markers of MSG epithelial cells were detected by confocal analysis using anti-MHC class II, CD86, CD80, ICAM-1 mAbs, anti-keratin polyclonal antibody, Alexa Fluor 568–conjugated anti-rat IgG (red), Alexa Fluor 488–conjugated anti-rabbit IgG (green), and DAPI (blue). Images are representative of five to seven mice. Bars: (A and C) 50 μm.

mice was observed compared with DCs from WT mice (Fig. 4 C). Approximately half of the T cells response to 10^5 DCs from *RbAp48*-Tg mice equaled the level of the response to 10^5 MSG cells from the Tg mice (Fig. 4, B and C).

Crucial role of epithelial IFN-γ production

The expression of MHC class II molecules is generally regulated at the transcriptional levels, including the transcription factor IFN regulatory factor (IRF)-1 (28, 29) and the class II transactivator (CIITA), which is the master regulator for MHC class II gene expression (30, 31). It has been shown that IRF-1 is a primary responsible gene of the IFN-γ response (32). In in vitro studies using human salivary gland (HSG) cells (33), IFN-γ–induced mRNAs of IRF-1 and CIITA were significantly enhanced by treatment with Tamoxifen (Tam), which is an antagonist of estrogen and can induce RbAp48 (23), or transfection of pCMV-*RbAp48* plasmid in the dose-dependent manner (Fig. 5 A), not in MCF-7 cells (human mammary gland cell line; Fig. S5, A and B, available at http://www.jem.org/cgi/content/full/jem.20080174/DC1). In addition, we next analyzed the IRF-1 promoter activity using *RbAp48*-transfected HSG cells with and without IFN-γ by luciferase assay. We observed significantly enhanced IRF-1 promoter activity in *RbAp48*-transfected HSG cells with IFN-γ, not in MCF-7 cells (Fig. 5 B). Surprisingly, in *RbAp48*-Tg mice, a prominent expression of IFN-γ was detected in salivary and lacrimal epithelial cells besides sporadically positive infiltrating cells of *RbAp48*-Tg mice, not WT mice (Fig. 5 C). These findings were observed mainly in the MHC class II$^+$ ductal epithelium adjacent to lymphoid infiltrates. Epithelial IFN-γ expression in the exocrine glands of *RbAp48*-Tg mice was up-regulated during the course of autoimmune exocrinopathy. Induction of IFN-γ expression may occur through many different types of stimulation, including cross-linking of cell-surface receptors and stimulation with cytokines, including IL-2, -12, and -18 (34). It has been demonstrated that IFN-γ synthesis is predominantly induced by stimulation with IL-18 (35). Consistent with a previous study (36), IL-18 expression was observed in salivary epithelial cells in *RbAp48*-Tg mice, not in WT mice (Fig. 5 D). Confocal analysis revealed that differential expression of IL-18 and IFN-γ was clearly observed, i.e., IL-18 mainly in the acinar cells and IFN-γ in the duct cells, within salivary epithelial cells from *RbAp48*-Tg mice, but not from WT mice (Fig. 5 D). Controls using isotype antibodies were shown in Fig. S4 C. Epithelial IFN-γ and IL-18 productions were confirmed by flow cytometry using MSG cells without immune cells from *RbAp48*-Tg, not from WT mice, whereas there was no difference in both IFN-γ and IL-18 expressions of cLN cells between WT and *RbAp48*-Tg mice (Fig. 5 E). Although the production of IL-18 in salivary gland cells was detected in a previous study (36), there has been no proof for IFN-γ production of salivary gland cells in any paper. Therefore, to confirm IFN-γ production of exocrine glands, detection of IFN-γ using tissue homogenates was performed. A high concentration of IFN-γ was detected in the tissue homogenates of lacrimal and salivary glands from *RbAp48*-Tg mice, compared with that from WT mice, by ELISA (Fig. S6 A). Furthermore, the detection of IFN-γ mRNA of MSG cells was performed by in situ hybridization using the RNA probe of mouse IFN-γ gene. A more intense signal for IFN-γ mRNA in duct cells of salivary glands from *RbAp48*-Tg mice was observed compared with that from WT mice (Fig. 5 F). As for the expression of BAFF, which is an inducer of IFN-γ in B cells, the expression of epithelial cells was undetectable in both *RbAp48*-Tg and WT mice (Fig. S7). In vitro studies using HSG cells demonstrated that the expressions of IL-18, IFN-γ, and MHC class II (HLA-DR) were observed

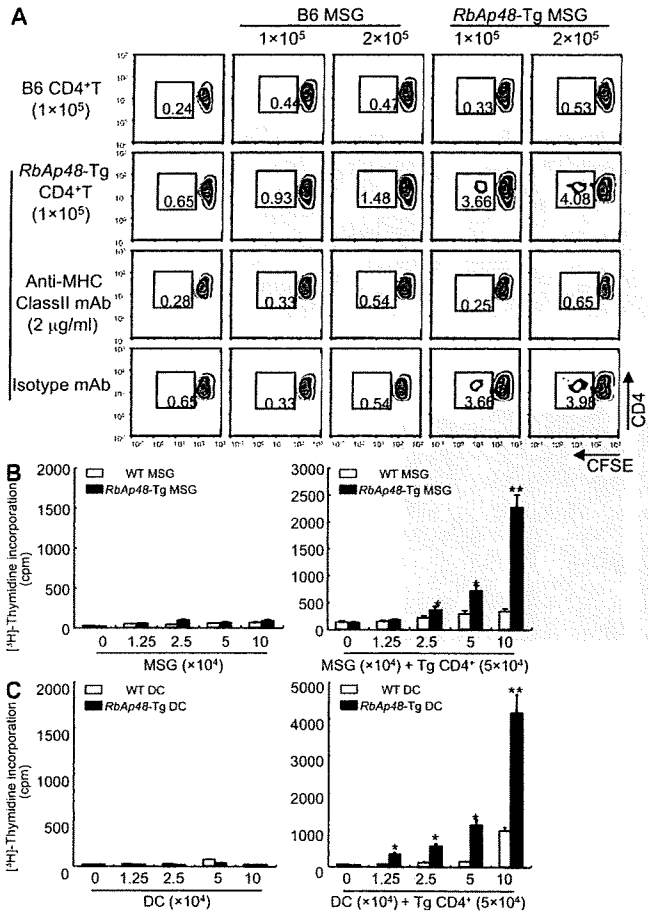

Figure 4. CD4$^+$ T cells can proliferate to epithelial cells from *RbAp48*-Tg mice. (A) CFSE-labeled purified CD4+ T cells (10^5) of WT and *RbAp48*-Tg mice were co-cultured with MSG cells (1 and 2 × 10^5) from the mice for 72 h. Cell proliferation was estimated by the dilution of CFSE. 2 μg/ml anti-MHC class II mAb or isotype control antibody was added in the culture. All results are representative of three to five mice at 28 wk of age, or three-independent experiments. (B) CD4+ T cells (5 × 10^4) of cLNs from *RbAp48*-Tg mice were co-cultured with irradiated MSG cells (0–10 × 10^4) from WT and *RbAp48*-Tg mice for 72 h. (C) CD4+ T cells (5 × 10^4) of cLNs from *RbAp48*-Tg mice were co-cultured with irradiated DCs (0–10 × 10^4) from WT and *RbAp48*-Tg mice for 72 h. Proliferative T cell response was evaluated by [^{3}H]thymidine incorporation during the last 12 h of the culture. Results are representative of means ± SE of triplicates in two independent experiments. *, $P < 0.05$; **, $P < 0.005$; WT versus *RbAp48*-Tg MSG cells or DCs.

Published November 24, 2008

when treated with Tam or transfected with pCMV-*RbAp48*, whereas they were inhibited when treated with 17β-estradiol (E2), caspase 1 inhibitor (Ac-YVAD-CHO; Ci), and siRNA of *RbAp48* (si; Fig. 6 A). Confocal analysis confirmed the expression of IL-18 and IFN-γ in HSG cells treated with Tam or transfected with pCMV-*RbAp48* (Fig. 6 B). It is important to note that IL-18 is secreted earlier (by 6 h) than IFN-γ production and HLA-DR expression (by 12 h) in Tam-stimulated and *RbAp48*-transfected HSG cells (Fig. S8). The most prominent function of IL-18 is its capacity to act as a potent costimulus for IFN-γ production (37–39). Indeed, we observed an increase in IFN-γ production in HSG cells treated with

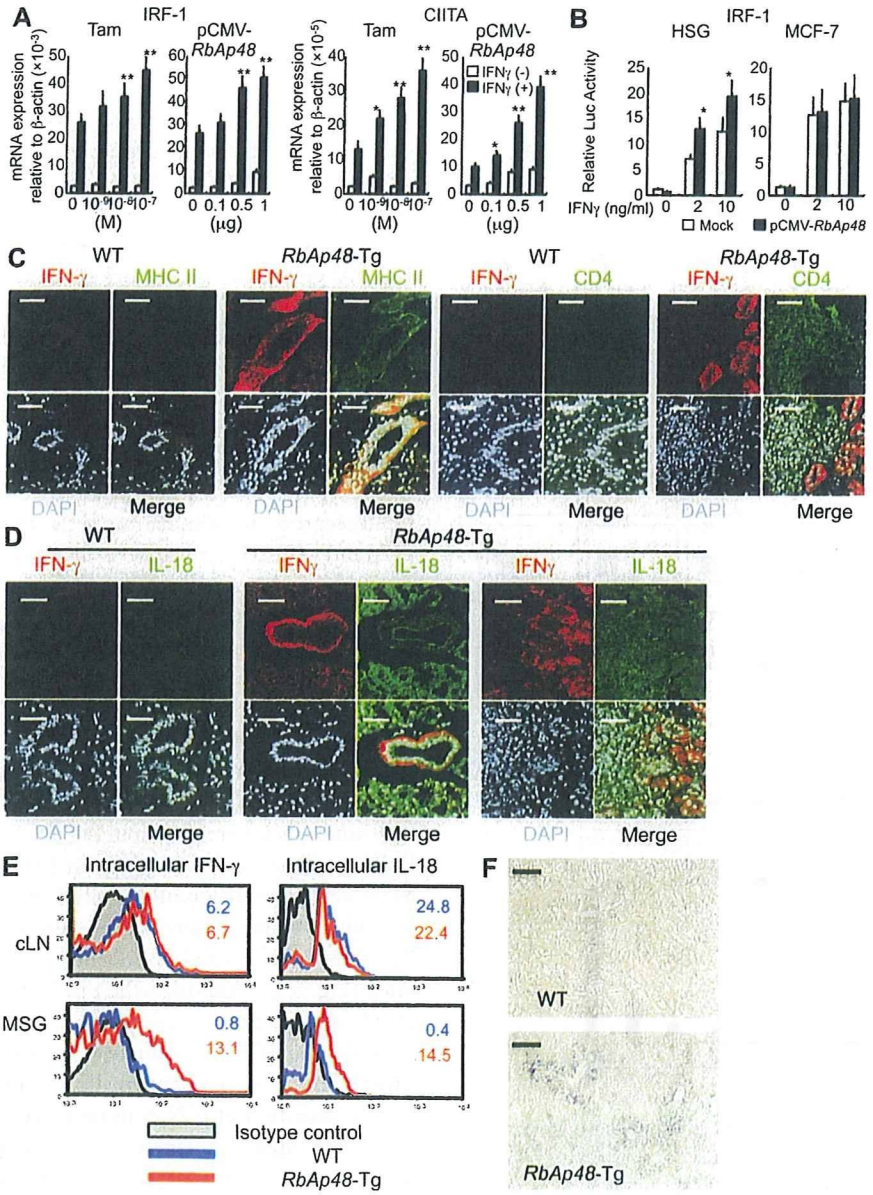

Figure 5. IFN-γ production from salivary epithelial cells stimulated with RbAp48. (A) IRF-1 and CIITA mRNA expressions of HSG cells stimulated with Tam (~10^{-9}–10^{-7} M) or transfected with pCMV-*RbAp48* (~0–1 μg) in the presence of IFN-γ (5 ng/ml) were detected by real-time PCR. Data are shown as means ± SE (SE) relative to β-actin mRNA of two independent experiments. *, $P < 0.05$; **, $P < 0.005$, versus IFN-γ (+) Tam 0 M or IFN-γ (+) pCMV-RbAp48 0 μg. (B) Promoter activity of IRF-1 in HSG and MCF-7 cells transfected with pCMV-*RbAp48*. Data are shown as means ± SE (SE) of two independent experiments. *, $P < 0.05$; **, $P < 0.005$, versus Mock (C and D) Confocal analysis of IFN-γ, MHC Class II, CD4, IL-18 or DAPI of salivary gland tissues from WT and *RbAp48*-TG mice at 32 wk of age. Alexa Fluor 488– or Alexa Fluor 568–conjugated anti-rat IgG were used as the second antibodies. Images are representative of three to five mice. (E) Intracellular IFN-γ and IL-18 expressions of cLN and MSG (without immune cells) cells from WT and *RbAp48*-Tg mice at 32 wk of age was detected by flow cytometric analysis. Results are representative and are shown as means ± SE of three mice of each group in two independent experiments. (F) The expression of IFN-γ mRNA in salivary gland cells of *RbAp48*-Tg mice was detected by in situ hybridization. Representative images of WT and *RbAp48*-Tg mice are shown in two independent experiments. Negative (antisense probe) or positive controls for mouse IFN-γ RNA probe are shown in Fig. S6 B. Fig. S6 is available at http://www.jem.org/cgi/content/full/jem.20080174/DC1. Bars: (C) 50 μm; (D) 40 μm.

recombinant IL-18 in the dose-dependent manner, but not in MCF-7 cells (Fig. S9, available at http://www.jem.org/cgi/content/full/jem.20080174/DC1), by ELISA and flow cytometry (Fig. 6 C). Confocal analysis of IFN-γ production of HSG cells in response to IL-18 together with cytokeratin as an identified marker was shown in Fig. 6 D. Moreover, we found a significant up-regulation of caspase 1 activity in lacrimal and salivary glands from *RbAp48*-Tg mice relative to that from WT mice (Fig. 6 E). In this regard, we reported previously significantly increased caspase 1 activity in salivary gland tissues from ovariectomized (Ovx) C57BL/6 mice in vivo (22) and Tam-stimulated and *RbAp48*-transfected HSG cells in vitro (23).

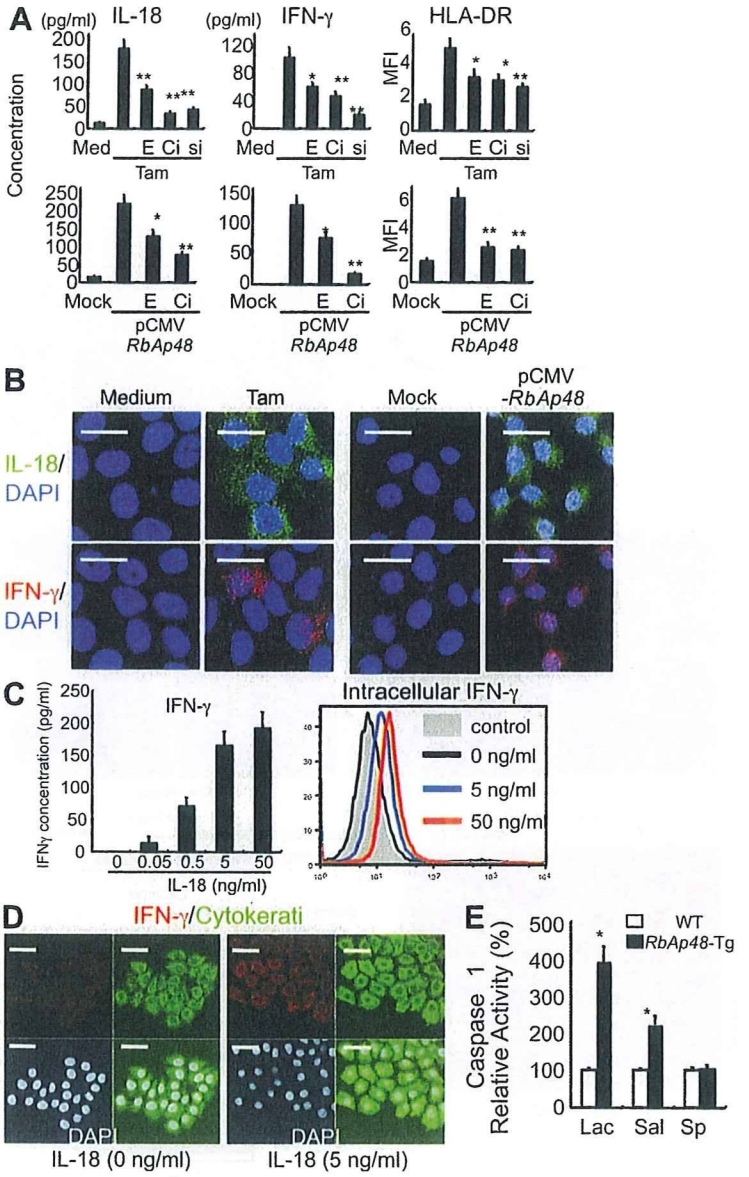

Figure 6. Expressions of IL-18, IFN-γ, and MHC class II (HLA-DR) in HSG cells when treated with Tam and transfected with pCMV-*RbAp48*. (A) Inhibitory effects of 10^{-9} M 17β-estradiol (E) or 10 μM caspase 1 inhibitor (Ci) on RbAp48-induced IL-18, IFN-γ, and HLA-DR in HSG cells. IL-18 and IFN-γ of the culture supernatants were detected by ELISA. HLA-DR is shown as mean fluorescence intensity (MFI) by flow cytometric analysis. *, $P < 0.05$; **, $P < 0.005$, versus RbAp48-induced. Data are means ± SD of triplicate samples, and representative of two independent experiments. (B) Tam- or RbAp48-induced IL-18 and IFN-γ were detected by confocal microscopic analysis. IL-18, IFN-γ mAbs, and Alexa Fluor 488– or Alexa Fluor 568–conjugated anti-mouse IgG were used. Images are representative of three independent experiments. (C) IFN-γ secretion or production of HSG cells by the addition of recombinant IL-18 was detected by ELISA or intracellular flow cytometric analysis. Data are representative of three independent experiments. (D) IFN-γ expression of IL-18–stimulated HSG cells was detected by confocal microscopic analysis together with cytokeratin and DAPI stainings. Images are representative of three independent experiments. (E) Caspase 1 activity of lacrimal, salivary glands, and spleen from *RbAp48*-Tg mice at 28 wk of age. Data are shown as means ± SE of four mice in two independent experiments, relative to those of WT mice. *, $P < 0.05$; **, $P < 0.005$; WT versus *RbAp48*-Tg mice. Bars: (B) 20 μm; (D) 50 μm.